ME 450 Design & Manufacturing III
Fall 2020 - Final Report
Team 27 - Thermal Inefficiencies

Section 07 - Professor Jyoti Mazumder
Section 03 - Heather Cooper
Project Sponsor - Professor Chinedum Okwudire

Michael Fanelli
Luthfor Khan
Jake Melvin
Stefan Milevski
Hao Wang

Executive Summary

This document serves as a final design report for Team 27 in ME 450 this semester. We have completed all necessary background research and built a constrained design space to better define and, by extent, solve the problems we have found in additive manufacturing. In particular, the additive manufacturing process we are interested in is the fused deposition modeling (FDM) of acrylonitrile butadiene styrene (ABS). After identifying thermal inefficiencies and discrepancies as the root cause of some types of deformation and failure in the printing process, we designed a testing procedure to gather background benchmark data for the printing failures that occur. We have also consulted with many stakeholders both in academia and in the industry to better understand what requirements they need on a solution. These requirements include warpage prevention, consistency, and quality of printed parts as well as a cost-efficient, spatial, and easy to setup solution. We compiled this information into a formative plan to design a solution for thermal inefficiencies with plans for testing and validation of our findings. The concept chosen to best meet these requirements includes a surrounding enclosure with various heating elements along the bed. To regulate the temperatures of the air in the enclosure and along the bed, a control system was installed. An ABS adhesive will also be used to help ground the part to the printing bed. This helps the part when it is most susceptible to warping at the beginning of the print. This combination of ideas provided the best means of providing a uniform temperature surrounding the part, a uniform temperature along the printing bed, and a uniform method of cooling given the time and cost constraints on our project. Having met with stakeholders, we determined a scaled approach to the design was necessary as to not increase the complexity of our control system. We tested the temperature regulation needs and set up phases of design. Considerable testing has been completed and our design with heating elements and an enclosure has been prototyped. We have determined that an ambient temperature does not need a convective controller since the added heating system and simple enclosure get the temperature to an adequate temperature range on its own. We have constructed an enclosure and conductive temperature control system on the bed. We then did extensive heat transfer modeling to verify the efficacy of our design. We finally competed printing parts and measuring their deviation to validate our solution's strengths in solving our framed problem.

Contents

1 Problem Definition

1.1 Introduction

Our ME450 team investigated some of the problems that arise due to thermal inefficiencies during the 3D printing process for polymers. Specifically, we are interested in analyzing these effects in the fused deposition modeling (FDM) of acrylonitrile butadiene styrene (ABS) filament. The goal of our project is to design and manufacture a low-cost solution that can either decrease these thermal inefficiencies or mitigate their negative effects. Our team consists of five seniors in mechanical engineering at the University of Michigan and our project sponsor is Dr. Chinedum Okwudire, an associate professor in Mechanical Engineering at the University of Michigan.

This semester our project had a limited budget of $500. Due to the timing of health-related concerns with COVID-19, our team looked for projects that could be done reasonably with as little in-person interaction as possible while staying within budget. Furthermore, all meetings were virtual with stakeholders and team members. To analyze these thermal inefficiencies in 3D printing and to follow the requirements stated above, we purchased an Ender 3 3D printer from Creality. The printer operated in one of our team member's living spaces.

1.2 Problem Definition and Background

1.2.1 Industry Research

The process of 3D printing consists of various types, and they all fall under a broader category of manufacturing called additive manufacturing (AM). These types include processes such as stereolithography (SLA), fused deposition modeling (FDM), and SLS (selective laser sintering). In the case of polymers, FDM is a common technique that has become rapidly more available in the world. The FDM process uses a nozzle to deposit melted polymer to form a structure in a layer by layer technique [1].

This manufacturing style allows for FDM to have many advantages compared to traditional manufacturing techniques. For example, FDM has lower setup costs than many other manufacturing processes due to the machinery required. FDM also offers the creation of unique shapes and structures, where processes like injection molding or machining will not work or might be too costly. These two properties allow FDM to be an ideal tool for prototyping.

Although, FDM has numerous drawbacks that prevent it from being widely deployed in industry. Quality is one of the most significant drawbacks. Even though FDM is mostly used for prototyping purposes, where dimensional accuracy and part quality are not critically important, industry users still found the quality of the printed parts lacking. Dave Veisz, the VP of Engineering at MakerBot stated, "To date, most desktop solutions cannot offer reliability and precision that is comparable to more expensive, larger industrial machines. As a result, many smaller businesses wouldn't even consider any form of in-house 3D printing as a viable option" in 2019[1]. Desktop FDM printers cannot produce parts with the reproducibility and repeatability of other traditional manufacturing equipment, such as milling and lathing machines. This disadvantage is a concern for industry users because it can lead to significant costs, safety concerns, and part failure. There are also other negative aspects of FDM, such as print times, material limitations, and shrinkage. Furthermore,

[1] Dave Veisz, "Price, Performance, Potential – Closing the Gap in 3D Printing," Society of Manufacturing Engineers, October 16, 2019, https://www.sme.org/price-performance-potential–closing-the-gap-in-3d-printing.

when a part is printed through FDM, it is known that the mechanical properties of the product are less than that of the original filament [2].

On the other hand, more capable industrial-grade FDM printers can offer better part quality and dimensional accuracy, but they are significantly more expensive than desktop FDM printers. Additionally, companies have to hire a team of skilled workers to operate and perform maintenance on the printer, and it does not make much sense to pay for an expensive machine and wages to just print prototypes. As a result, a lot of industry users outsource their FDM printing jobs, even though the cost per part is drastically higher. When choosing which 3D printing service provider to outsource their parts too, 34% of companies view quality as the most important criterion[2].

As discussed previously, many companies do not have in-house 3D printing due to the printer's lack of precision and quality. Not surprisingly, when they outsource jobs to service providers, quality is very important to them. Furthermore, as more and more companies choose to have their own in-house 3D printing capabilities quality and process control are rising in importance. Jabil, a large manufacturing services company, surveyed in 2017 and 2019 industry users of 3D printing, asking them what their greatest challenges were. In 2017, the part quality was the fourth biggest challenge, but in 2019, it became the second biggest challenge behind only the cost of materials[3]. As a growing number of companies view spare parts production as a growth opportunity for additive manufacturing, both customers and suppliers of service parts view part quality as the fourth biggest challenge, according to a PricewaterhouseCoopers report[4]. The top two challenges, technical maturity/feasibility and 3D printing know-how, will likely resolve themselves over time as 3D printing becomes more ubiquitous in manufacturing processes. However, other challenges they cite, such as available materials, manufacturing costs, and product quality require some technical innovation.

1.2.2 Stakeholder Input

1.2.2.1 Project Sponsor: Dr. Chinedum Okwudire

Our initial investigation into this problem started with our first meeting with our project sponsor, Dr. Okwudire. Our discussion revealed that 3D printers have many flaws, and one of them is an issue with thermal-induced deformations in polymer extrusion. To show that we can reduce these deformations, we needed to focus on the consistency and predictability of the printed parts.

Dr. Okwudire also mentioned that he had information from a previous research project. To summarize, his past project determined that different 3D printers have different characteristics and, depending on the 3D printer model used, the printing bed may not have a uniform temperature. It was found that this temperature variation on the build plate had affected the degree of warping in the parts. This is a case of thermal-induced inefficiencies and one we would like to further explore.

[2]Frank Thewihsen et al., "If 3D Printing Has Changed the Industries of Tomorrow, How Can Your Organization Get Ready Today?," Ernst amp; Young, 2016, https://www.ey.com/Publication/vwLUAssets/ey-3d-printing-report/$FILE/ey-3d-printing-report.pdf.

[3]Geoffrey Doyle, "Top 3D Printing Problems and Solutions," Jabil, August 15, 2019, https://www.jabil.com/blog/overcoming-top-3d-printing-challenges.html.

[4]Reinhard Geissbauer, Jens Wunderlin, and Jorge Lehr, "The Future of Spare Parts Is 3D," Strategy&; (PricewaterhouseCoopers, 2017), https://www.strategyand.pwc.com/gx/en/insights/2017/the-future-spare-parts-3d/the-future-of-spare-parts-is-3d.pdf.

1.2.2.2 Stakeholder Outreach

We sought out external stakeholders that have industry experience in polymer additive manufacturing, were subject matter experts in the field, or both. We reached out to Deere Company, Ford Motor Company, and General Motors on the industry side. At the University of Michigan, we also spoke to Ph.D. students and professors in manufacturing engineering and materials science engineering. Each stakeholder had a unique perspective, but some key themes ran through our stakeholder interviews. The most important was consistency. Some stakeholders referred to this as consistency, while others talked about reproducibility, repeatability, and predictability. These stakeholders stressed a desire to be able to achieve consistent results for a common set of build parameters or conditions as one of the common challenges for 3D printing is variability in parts that are printed under very similar conditions. The second main takeaway from these interviews was the prioritization of precision over accuracy. Our stakeholders would much rather have a precise dimension that is very repeatable than one that is accurate but varies a lot. Prof. Okwudire used the analogy of a watch. Most people would prefer a watch that is always 5 minutes early than a watch that gives the correct time on average but can be five minutes late or five minutes early. Our industry stakeholders also stressed a low-cost approach, even despite the large size of their companies. There is a resistance to large fleets of expensive industrial printers, and our stakeholders desire a desktop 3D printing solution that is cost-efficient and high-performing. Finally, our stakeholders stressed the need for the structural integrity of printed parts. One of our stakeholders explained that, for a 500-layer part, there are 500 new points of failure that wouldn't exist if the part was injection molded. While 3D printed plastic parts won't reach the material properties of injection-molded plastic parts in the near future, any improvements in material properties would satisfy a major need. These external stakeholder interviews provided us with valuable insights from many different perspectives.

1.2.3 Literature Review

1.2.3.1 Warpage

Filament materials that have high thermal expansion coefficients are prone to warping in the FDM printing process. On the micro-level, warping and some other common 3d printing defects, such as layer separation and splitting, are caused by weak interlayer bonding [3] [4]. A large number of papers have dedicated much attention to the bond strength between layers and how it affects the quality and mechanical properties of the print [5] [6] [7]. However, we are going to handle the problem at the macro-level, meaning that this project will focus on process parameters that we can control instead of investigating the micro-level interactions within the part.

In the paper written by Wang et al. [8], the researchers proposed a mathematical model of warpage of ABS during the FDM printing process. They determined that the amount of warpage is affected by the following factors: chamber temperature, stack section length of the part, linear shrinkage rate, and the glass transition temperature of the filament material. Based on the proposed model, the authors concluded that higher chamber temperature and shorter stack section length of the part can help reduce warping for ABS. The paper also mentions that warpage is primarily a result of inner stress accumulated during the cooling process. Specifically, the most amount of inner stress is introduced during the cooling process from the glass transition temperature to the chamber temperature, and this process happens quickly [9].

Similarly, Turner et al. mentioned in their paper [10] that warping in Fused Deposition Modeling (FDM) printed parts is primarily caused by uneven temperature gradient within the part. In high-end 3D printers, the uneven temperature gradient problem is addressed by raising the chamber temperature (temperature-controlled oven). However, for lower-end 3D printers, the problem is only partially addressed by incorporating heat build platforms, which helps initial layers to adhere to the platform better. Another approach to ameliorate an uneven temperature gradient of the part is proposed by Ravoori et al. [11]. The authors proposed to attach a heated block of constant temperature near the nozzle which helps improve the temperature uniformity of the top layer of the part before and after filament deposition.

Lastly, the degree of deformation is a piecewise function of the conditions. Before reaching the onset condition, the part will not warp. However, once the onset condition is reached, the corners of the part would lift off the bed and warpage begins. As a result, we can prevent warping by preventing the corners of the part from lifting off the bed in the first place.

1.2.3.2 FDM Process Parameter Study

A study was performed analyzing how variations in 13 various process parameters in FDM affected both geometric (e.g., flatness, straightness, perpendicularity) and dimensional (e.g., length, width, height) accuracy [12]. These parameters included various factors, such as component size, infill parameters, and temperature parameters. A test component was proposed that met basic criteria such as low print time, basic geometry, and easy to measure. The test components in the study were printed with 1.75 mm diameter ABS.

Testing included the use of a coordinate measuring machine (CMM) to evaluate the test part for both dimension and geometric characteristics. In terms of thermal related parameters, it was found that the extruder temperature had the fifth-highest significance in affecting dimension and the highest significance in affecting geometric characteristics. The platform temperature had the second-highest significance in affecting dimension.

As a result, we believe the extruder and platform temperatures have a great impact upon the cooling of the filament along with the ambient temperature, and we believe this cooling process will also affect both the dimension and geometric properties of FDM printed ABS parts.

1.2.3.3 Heat Transfer Phenomena

Modeling the temperature of the FDM process is very complicated as there are many modes of heat transfer present in the system. Namely, as the first filament is placed, heat is transferred by conduction from the bottom layer of the filament with the printing bed, convection with the ambient air, and radiation with the surroundings [2]. Conduction heat transfer then arises between layers when the layers are deposited next to and above the previous filaments. This process also creates very small amounts of trapped air in which convection and radiation can occur between the layers [13]. An example model including these parameters can be seen in Figure 1a. There is another mode of heat transfer associated with the melting and solidification of the polymer. This melting can lead to a melt pool that would add another form of convection to the model affecting the temperature gradient as well as the surface deformation. However, due to the time constraint for this project, this effect was, unfortunately, ignored for any calculations.

A study analyzing these effects determined that the most significant modes of heat transfer occurred with convection to the environment and conduction between the layers and printing bed [13]. In particular, it was found that when the convection coefficient of the ambient air was above 60 $\frac{W}{m^2K}$ the radiation effects with the surroundings could be neglected. Also, it was determined that the convection and radiation effects between the layers can be ignored. This leads to a simplification of the previous model with the dominant modes of heat transfer shown in Figure 2.

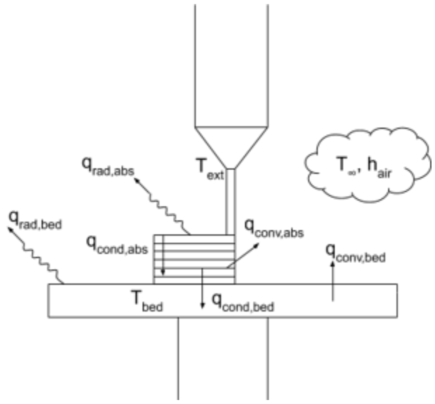

(a) FDM heat transfer model showing the various modes of heat transfer present in the system.

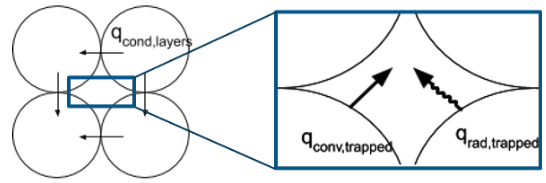

(b) Radiation heat transfer and convection heat transfer occurring in the small air gaps between layers.

Figure 1: Heat transfer models.

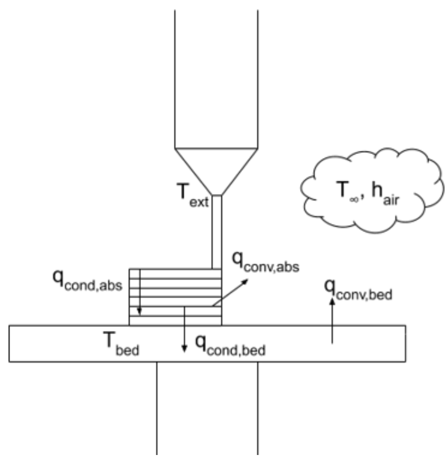

Figure 2: Simplified heat transfer model showing only the dominant modes of heat transfer present in our system.

To further understand the model shown above, there are some governing heat transfer equations that can be useful to address. The first being the conduction rate equation (Fourier's Law) for a one-dimensional planar wall:

$$q''_{cond} = -k\frac{dT}{dx} \tag{1}$$

where q_{cond} is heat flux ($\frac{W}{m^2}$), k is the thermal conductivity of the material ($\frac{W}{mK}$), and $\frac{dT}{dx}$ is the temperature gradient in the x direction ($\frac{K}{m}$) [14]. Fourier's law can also be written in a more general form for three dimensional applications:

$$q''_{cond} = -k\nabla T = -k(\mathbf{i}\frac{dT}{dx} + \mathbf{j}\frac{dT}{dy} + \mathbf{k}\frac{dT}{dz}) \tag{2}$$

where q''_{cond} is the heat flux ($\frac{W}{m^2}$), k is the thermal conductivity of the material ($\frac{W}{mK}$), is the three-dimensional del operator, the vectors **i**, **j**, and **k** are the unit vectors, and T(x, y, z) is the scalar temperature field [14]. This equation can be used to formulate the 3D heat diffusion equation to see the temperature distribution throughout a medium:

$$\frac{\partial}{\partial x}(k\frac{\partial T}{\partial x}) + \frac{\partial}{\partial y}(k\frac{\partial T}{\partial y}) + \frac{\partial}{\partial z}(k\frac{\partial T}{\partial z}) + \dot{q} = \rho c_p \frac{\partial T}{\partial t} \tag{3}$$

where k is the thermal conductivity of the material ($\frac{W}{mK}$), $\dot{q}$ is the energy generated per unit volume of the medium ($\frac{W}{m^3}$), ρ is the material density ($\frac{kg}{m^3}$), and c_p is the specific heat with constant pressure ($\frac{J}{kgK}$) [14]. The above equations can be used to analyze how conduction heat transfer takes place between the layers and between the layers and the build plate. To analyze the other significant mode of heat transfer in the system, convection, we can use Newton's Law of Cooling:

$$q''_{conv} = -h(T_s - T_\infty) \tag{4}$$

where q_{conv} is the heat flux ($\frac{W}{m^2}$), h is the convection heat transfer coefficient ($\frac{W}{m^2K}$), T_s is the surface temperature (K), and T_∞ is the ambient fluid temperature (K) [14]. These equations will interact with each other differently depending on the geometry of the part, where the part is printed, at what section of the part is being printed, and many more factors. This results in a transient problem with many moving pieces and changing variables. To best get an estimate of what the temperature gradient is, a simulation will be constructed.

1.2.4 Problem Description

After discussions with our sponsor, various stakeholders, and consulting past literature, we have concretely defined the design problem. Namely, there are thermal-induced geometric deformations when FDM printing with ABS due to temperature variations between printed layers and among the build plate as well as uneven cooling of the printed parts. Which can lead to adverse effects such as warping on part edges and inconsistency in part dimensions.

Our project goal is to design and manufacture a low-cost solution to these thermal-induced deformations. If this goal is successful, we could provide a solution to industry users that would enhance the quality of their desktop 3D printers.

1.3 Requirement and Specifications

After interviews with stakeholders and literature review, we condensed the information obtained in the process down to six requirements. Three of the requirements are related to the quality of the 3D printed parts, and the remaining requirements pertain to other aspects, such as cost and spatial dimension. The summary of requirements and specifications are given below in Table 1.

1.3.1 Warpage Prevention

Fused deposition modeling (FDM) is not known for its dimensional accuracy or print quality. Although mitigation techniques have been actively explored for the past decade, FDM still has some severe limitations on dimensional accuracy. Unlike shrinkage, a common but relatively benign form of dimensional deviation, warpage is often catastrophic and can render a part useless. Materials that have a high thermal expansion coefficient, such as ABS, are more prone to warping than materials with a lower thermal expansion coefficient [8]. Even though materials like ABS are more prone to warping, they are widely used as prototyping materials in the manufacturing sector because of their superior mechanical properties. As a result, reducing warpage in FDM for materials like ABS has numerous benefits including improving part quality, reducing cost, and shortening development cycles, etc.

Table 1: Stakeholder Requirements and Engineering Specifications.

Stakeholder Requirements	Engineering Specifications
Warpage Prevention	The dimension at each corner of the test part should not deviate more than 20% from the median corner dimension.
Consistency	The standard deviation of the corner height measurements should be less than 5% of the mean corner height dimension.
Quality	First pass yield of above 90%
Cost Efficiency	Production cost must be below Creality's current $90 product, and prototyping cost must be below $200.
Spatial	Solution cannot extend the envelope of the 3D printer more than 20% in the two directions in the plane of the table.
Ease of Setup	Assembly instructions must be accessible, and the number of parts must be limited so that the system can be assembled in under 60 minutes.

Warpage is induced by thermal stress induced in the process of uneven cooling, and corners of the part are the most affected areas. Hence, we quantify warpage by the dimensional deviation of the corners[5] of the part. The engineering specification that corresponds to this stakeholder requirement is that the dimension at each corner of the test part should not deviate more than 20% from the median corner dimension.

1.3.2 Consistency

Apart from dimensional inaccuracy, FDM also suffers from consistency issues, which can be attributed to several factors, such as shrinkage, warpage, and layer adhesion quality. Dimensional deviations that result from shrinkage are generally predictable because the shrinkage of a material can be roughly calculated from the part's dimension and thermal expansion factor. On the other hand, dimensional deviation caused by warpage is more unpredictable, and some researchers have proposed warpage prediction models [8]. For a series of printed parts, precision is more important than accuracy because precise parts can be more easily compensated for dimensional deviation by introducing a fixed offset.

For this requirement, we will continue to use the dimension of corners to quantify the effectiveness of our solution, and we will measure the deviance in the corner dimension using standard deviation. The engineering specification corresponds to this requirement is that the standard deviation of the

[5]In this case, dimensional deviation = design corner height - actual corner height

corner height measurements should be less than 5% of the mean corner height dimension. The 5% used in this specification is an estimate we arrived at after reviewing the initial testing data. The standard deviation calculated using initial testing data is about 3%, which we believe is an underestimate due to the lack of available testing parts[6].

1.3.3 Quality

It was mentioned during an interview with one of our stakeholders from the manufacturing industry that their 3D printed parts have about a 90% catastrophic failure rate, which indicates functionally unusable parts. A catastrophic failure can stem from several failure modes or combinations of them. For example, severe warpage can be categorized as a catastrophic failure because the part does not meet dimensional requirements and is considered unsalvageable. Similarly, layer separation and shifting can also be considered catastrophic failure modes. The aforementioned failure modes are serious quality concerns, and we want to address them through our proposed solution.

The engineering specification for this requirement is quantified using a first pass yield rate. As we have mentioned above, one of the stakeholders is experiencing a catastrophic failure rate of 10%, and we would like to reduce that below 10%. As a result, we would like to have a first pass yield of above 90%.

1.3.4 Cost Efficiency

Even though the cost for a low-end FDM printer has gone down significantly over the years, an industrial-grade 3D printer is still very costly. Considering that FDM is primarily used for rapid prototyping, many companies are not looking to heavily invest in FDM printers or use them frequently. The price can sometimes be a deciding factor for some of our stakeholders. As a result, our stakeholders want our solution to be low-cost.

There are existing solutions designed to address the thermal-induced deformation/dimensional deviation. Notably, Creality designs a thermal cover for its Ender 3 3D printer and it is marketed at 90 dollars. We want our solution, if it enters the market, to have a lower price tag, although the prototype cost for our solution can be higher. Hence, the engineering specification for this requirement is that the prototyping cost of our solution to be below 200 dollars and the production cost must be below the $90 benchmark.

1.3.5 Spatial

Many stakeholders are looking to utilize desktop FDM printers, and they want the printer, along with our solution prototype, to be relatively compact and space-efficient. Hence, the engineering specification for this requirement is that our solution cannot extend the envelope of the 3D printer more than 20% in the two directions in the plane of the table.

1.3.6 Ease of Set Up

Some stakeholders also expressed concerns in the setup process of FDM printers. Most FDM printers are integrated systems that are easy to set up, but fine-tuning the bed level and pre-heating filaments can take up some substantial amount of time (60 minutes). They want our solution to be easily set up in a short amount of time. The engineering specification for this requirement is

[6] We only had nine initial testing parts

that assembly instructions must be accessible, and the number of parts must be limited so that the system can be assembled in under 60 minutes.

2 Concept Exploration

2.1 Concept Generation

After our problem definition, stakeholder requirements, and engineering specifications were well-defined, we entered the concept generation phase in the concept exploration stage of the design process. We began our exploration of the design solution space with a 90-minute brainstorming session. Due to COVID-19 health-related concerns, this brainstorming session occurred online using Microsoft Whiteboard as our collaborative medium. Following brainstorming guidelines, we deferred judgment of suggestions and practiced divergent thinking. This allowed us to explore a wide and diverse solution space. We initially came up with over 70 unique, potential solutions and categorized the solutions into three categories: mechanical, thermal, and electrical. During and after the brainstorming session, we organized our ideas into the mind map presented in Appendix A in Figure A1. This mind map allowed us to better visualize our design space.

2.2 Concept Development

As we moved into the concept development phase, we conducted an initial screening of our 70+ brainstormed ideas to create a more manageable set of ideas to develop further. We classified each of our ideas from the brainstorming session as feasible, somewhat feasible, and not feasible for the scope of this project with the constraints that we have. These categories corresponded to green, yellow, and red shading, respectively. This depiction can be seen in the Appendix in Figure A2. Ideas colored in red were deemed not feasible due to certain characteristics such as high cost, safety concern, limited resource access, or limited effectiveness. For example, using nuclear fission to heat water as a heat source for our solution would have major cost and safety concerns. Another idea deemed not feasible was the idea of increasing the size of the 3D printer. This idea may have benefits to the quality and consistency of parts; however, it does not satisfy some of our requirements as this would increase the spatial aspect of the printer. After creating a more manageable set of ideas to expand and iterate in the concept development phase, we created a new, smaller mind map, as seen in Figure 3.

To further expand the design space, the first tool we used was Design Heuristics [15]. Using various design heuristic cards allowed us to generate more solutions. For example, after looking at the "cover or wrap" heuristic card, we thought about the possibility of printing a surrounding wall about the part. This wall would create a small enclosure around the part that could help standardize the temperature around and throughout the part. Another card we used was the "change surface properties" card, prompting us to think about the possibility of perforating the printing bed. The perforations would allow the use of a vacuum system below the bed to help adhere the parts to the bed or allow the use of a heat pump from underneath.

Before we advanced to the next stage of concept development, we decided to screen concepts a second time to create a more manageable morphological chart. At this stage, some design concepts were eliminated because more than one design solved the same problem or some design concepts were more effective when combined. Others might have caused an excessive change to the surrounding environment, including temperature and moisture, or posed a high risk if implementation failed, necessitating the purchase of a 3D printer or expensive replacement parts. For example, one idea

Figure 3: Mind map showing concepts we screened to be considered feasible or somewhat feasible for the scope of the project.

was to heat the room instead of creating a closed system in the 3D printer and heating that. This would be an inefficient use of energy and make the room very uncomfortable. After this screening process, we created a morphological matrix by identifying critical functions that all designs must achieve. These included standardizing the temperature throughout the build plate, standardizing the temperature throughout the part, cooling the part by lowering external surfaces at a steady rate, and adhering the part to the build plate. The remaining designs were neatly sorted into categories based on which function they served, as seen in the completed morphological matrix in Table 2. In doing so, we allowed ourselves to select multiple design sub-solutions to fully control the parameters that affect part deformations. These design subsections were grouped into candidate designs that are depicted and described below. Although there were 500 possible combinations of these design solutions, we selected three combinations to be our three candidate solutions.

2.2.1 Candidate Design #1

The First Candidate Design, as shown in Figure 4, combines several solutions, namely, a conductive build plate, a 3D printed part enclosure, ABS adhesive, and a heat sink. These would all work in conjunction to regulate the heating and cooling of the part. For example, the ABS adhesive would be applied to the bed before the print to allow for better adhesion between the part and the printing bed in the part's infancy when it is most fragile and susceptible to failure. Then, the enclosure would be printed with the part and act as a thermal barrier keeping the part insulated and near the glass transition temperature. Additionally, the enclosure will help deplete the effect of

Table 2: Morphological Matrix.

Function	Standardize temperature throughout build plate	Standardize Temperature throughout part	Cool Part by lowering external surfaces at a steady rate	Adhesion
1	Very strong convection heating element above 80°C	Print surrounding walls around the part	Submerge printed layer sin temperature-controlled fluid	ABS adhesive
2	Use a build plate material with a higher thermal conductivity	Enclosure around entire 3D printer	Controlled convection heat transfer/cooling	Vacuum system
3	Place multiple heating elements on build plate	Convection source (air, water, or oil flow)	Heat Sink	Print a raft
4	Install copper plate below existing printed bed to distribute heat from heating elements	Radiation source (heat lamp, etc)	Fans	No adhesion
5	Thermal paste with high conductivity	Controlled convection and bed heat pushing part towards same temperature	Perforated bed with Cooling pump	

the heating gradient of the bed on the corners of the workpiece. Lastly, a heat sink would be placed near the bed to reduce the ambient temperature around the part without warping the part. One advantage of this design is that higher thermal conductivity in the build plate would lead to more uniform temperature distribution. Additionally, surrounding the part with walls would create a small enclosure and decrease warping on the part itself. By trapping air in between the 3D printed wall and part, this design would be taking advantage of a good, natural, abundant insulator. However, a different build plate could be very costly and affect the removability of printed parts. Also, printing walls around the part would lead to increased waste material and print times.

2.2.2 Candidate Design #2

The Second Candidate Design, as shown in Figure 5, focuses on heating control over radical design changes. This design includes the addition of a plate with greater thermal conductivity, a controlled convection system for heating and cooling, and ABS adhesive. In this setup, a conductive copper plate is attached below the build plate. The copper plate has a higher thermal conductivity than the current aluminum plate to help achieve a more uniform temperate gradient along the surface of the printing bed. Furthermore, a controlled convection system is installed onto the build plate heating module to control the bed heating. This would lead to a more uniform bed heating gradient and pattern. A problem associated with this design is the complexity of trying to control the temperature near the middle of the printer and at the edges.

2.2.3 Candidate Design #3

The Third Candidate Design, as shown in Figure 6, that we constructed was rather ambitious. It features multiple heating elements along the edges of the build plate and an enclosure around the 3D printer. Moreover, the design includes a combination of a vacuum system with a perforated bed. The vacuum would create a suction adhering the part to the printer bed and act like a cooling

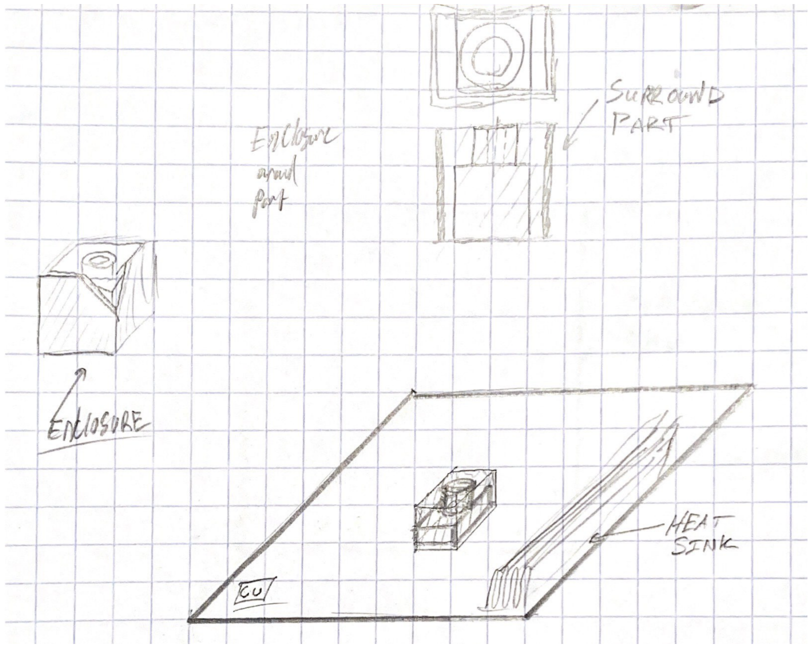

Figure 4: Sketch of Candidate Design 1.

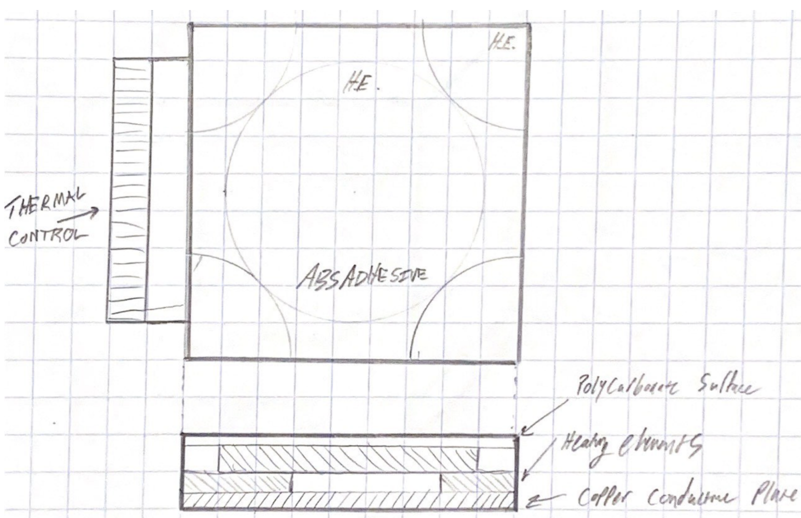

Figure 5: Sketch of Candidate Design 2.

pump. A problem with this concept is that there are many interacting components due to the vacuum element. There would need to be high precision when creating the solution as we do not want filament to be sucked below the printing bed or deform the part in any way. Also, the solution itself would require a lot of disassemblies and the installation of a new system in a 3D printer. As a result, this type of solution might be one to explore in the creation of a new 3D printer.

2.3 Concept Evaluation/Selection

2.3.1 Initial Testing and Modeling for Build Plate.

Before we evaluated our candidate designs, our team carried out initial testing to validate and quantify our problem. The objective of our initial test was to quantify the temperature variation

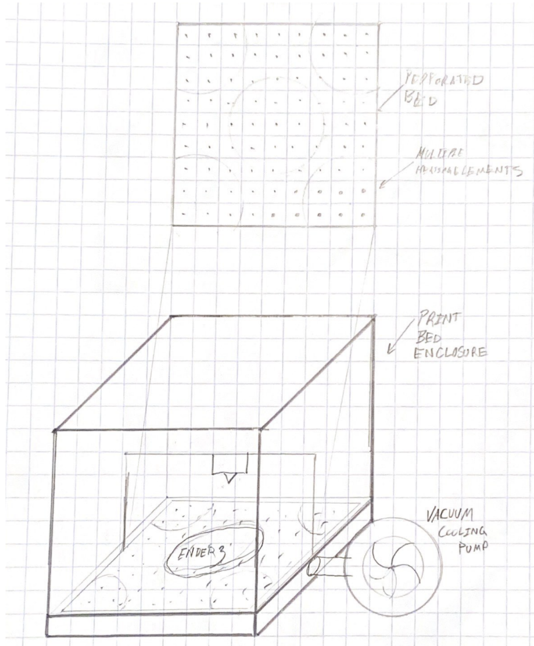

Figure 6: Sketch of Candidate Design 3.

among the build plate. We divided the build plate into nine equal regions and attached a thermistor to the center of each region to measure the temperature values. Additionally, a tenth thermistor was added to read the ambient temperature. The values of the thermistors were read real-time by an Analog-to-Digital Converter (ADC) shield attached to an Arduino UNO, and the data was then logged with a Raspberry PI Zero. A schematic of the setup is shown below in Figure 7.

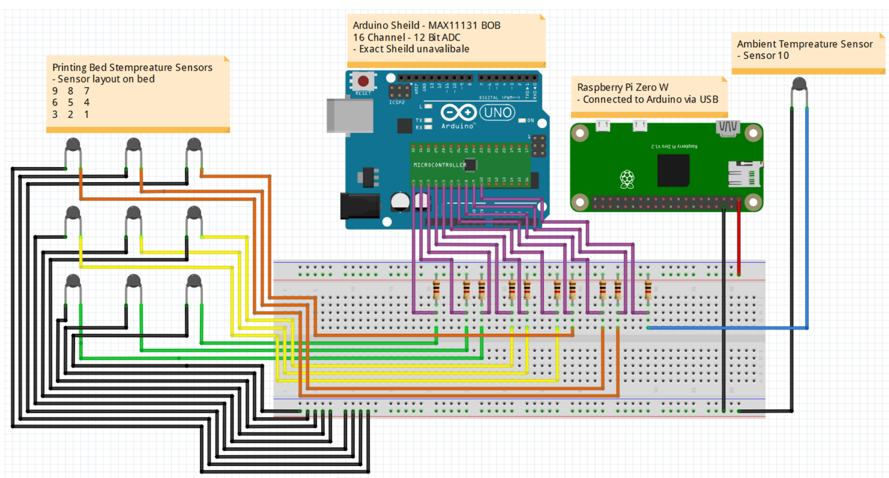

Figure 7: Temperature Data Acquisition Wiring Diagram.

To conduct the experiment, the 3D printer was left unused for a sufficient amount of time to reach a uniform steady-state temperature close to the ambient temperature of 20°C. The thermistors measured the temperature from the moment the 3D printer began to heat the print bed to the time after which they reached a steady-state temperature. The results are shown below in Figure 8.

As seen in Figure 8, the steady-state temperatures of the build plate regions varied considerably. In comparison to the set temperature of 90°C, the temperatures in the build plate regions dropped to as low as 73°C, creating a variation of nearly 20°C. This confirms our research that variations

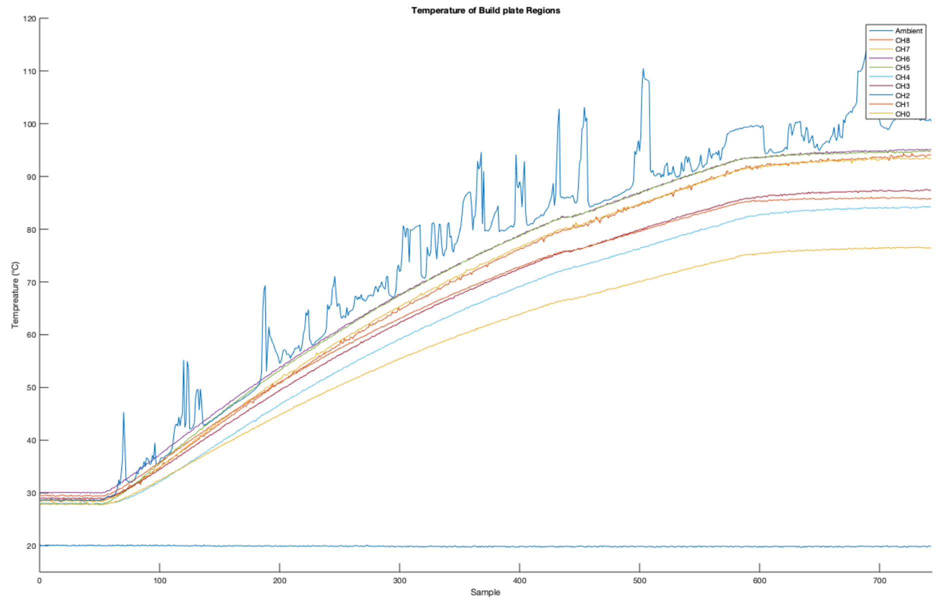

Figure 8: Measured Temperature of the 9 Regions of the Print Bed and Ambient Temperature.

in build plate temperature are significant and contribute to a lack of precision among the same printer, depending on where on the build plate the part was printed.

When considering possible solutions to a lack of uniformity in build plate temperature, our team considered adding a material with a high thermal conductivity between the heating element and the polycarbonate material. We intended to spread the heat from the heating element more evenly throughout the build plate. However, before building a physical prototype and testing the design, we first validated this design using the modeling software COMSOL Multiphysics. We created an assembly very similar to the one in the Ender 3 3D printer: a polycarbonate surface, an aluminum plate below that, and a heating element situated under the aluminum. This configuration is an approximation, knowing that the real-world system has a heating element under the aluminum plate that provides non-uniform heating with a single sensor in the middle of the build plate. Because of these approximations, we first established a benchmark for the temperature distribution according to the model under current conditions and ambient convection. Although this temperature variation among the build plate is not as extreme as in the experiment above, it provided a baseline for comparison when adding a copper plate between the polycarbonate top layer and the aluminum. In Figure 9 below, the left pane shows the baseline temperature distribution after reaching steady-state after 10 minutes while the right pane shows the temperature distribution with the copper plate. As shown in the scales, red indicates cooler surfaces while yellow and white indicate hotter surfaces.

As shown in Figure 9, the copper does make the temperature distribution more even, although the improvement is somewhat marginal. While the above figure describes the effect of Candidate Design #2's build plate solution on the temperature uniformity, we wanted to see the effects of combining the build plate solutions of Candidate Designs #2 and #3: inserting a copper plate between the aluminum and polyurethane and having multiple heating elements. We decided to place the heating elements at the four corners of the plate and observed the following results in Figure 10.

In this case, the copper plate caused the temperature distribution to decrease in the center of

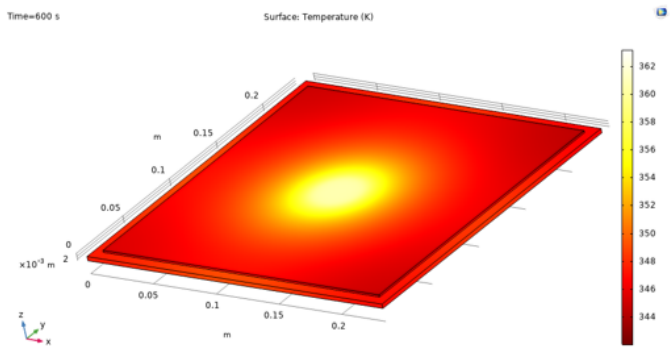

(a) No copper plate model.

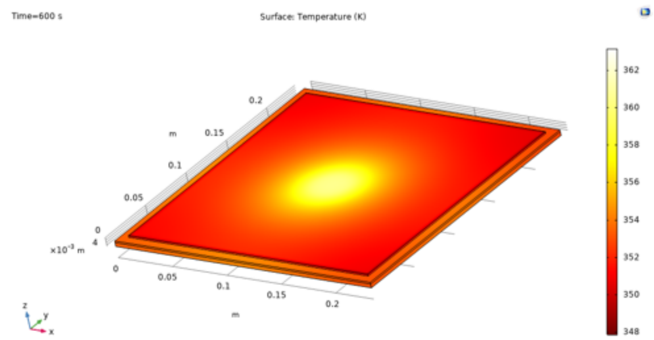

(b) Additional copper plate model.

Figure 9: COMSOL thermal models of build plate variations with a single heating element in the center.

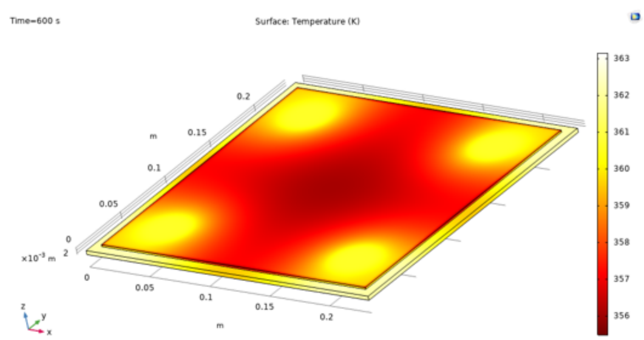

(a) No Copper Plate Model.

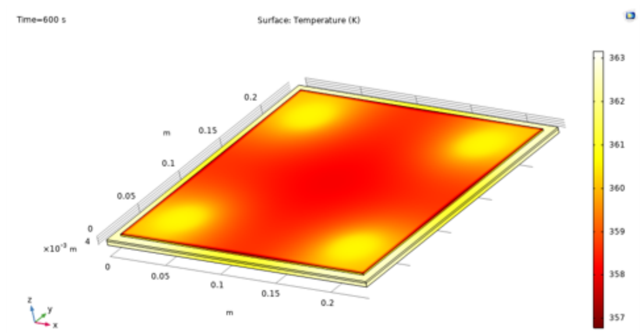

(b) Additional Copper Plate Model.

Figure 10: COMSOL Thermal Models of Build Plate Variations with Four Corner Heating Elements.

the plate as well. However, the temperature variation among the build plate decreased from 7°C to 4°C, a marginal benefit. These underwhelming results can be explained through the two competing effects of adding the copper plate: increased thermal conductivity and increased thermal resistance. Although copper is a highly conductive material with thermal conductivity of 385 $\frac{W}{mK}$, it also adds a thermal resistance that was not present previously, impeding the rate of heat transfer. Since the thermal conductivity of the aluminum plate is already relatively high at 205 $\frac{W}{mK}$, the copper plate doesn't provide as much of a thermal conductivity benefit over aluminum compared to the additional thermal resistance it provides. This explains the marginal benefits of the copper plate in Figures 9 and 10. For this reason, our team decided to move away from an additional copper plate heating in our selected solution.

2.3.2 Evaluation of Candidate Designs

In order to evaluate the candidate designs previously mentioned, we used a Pugh Chart. The chart used can be seen in Table 3. The metrics used to evaluate the designs were derived from our stakeholder requirements and engineering specifications. In the previous literature review and stakeholder meetings, we learned that two important contributing causes of warping are uneven printing bed temperature and low ambient temperature [8]. To reduce the thermal-induced warpage, increase consistency among parts, and increase the quality of the printed parts, we must keep the temperature of the parts constant, just below the glass transition temperature, as well as maintain a uniform high temperature throughout the print bed. Thus, we decided that the part and bed temperature will be weighted higher than the other categories. Furthermore, we also added metrics for uniform cooling and adhesion strength to the Pugh chart since they are beneficial to part quality and warpage reduction. The following rows include some design requirements themselves. To weigh our chart, our team took the emphasis placed on certain requirements from stakeholders and accordingly weighted how meeting each metric would help achieve the desired effect.

Table 3: Pugh chart

Metrics	Weight	Design 1	Design 2	Design 3
Maintain stable temperature throughout build plate	4	0	+1	+2
Maintain stable print chamber temperature	5	0	+1	0
Cool printed part at steady rate	3	0	+1	+1
Provide adhesion between build plate and part	3	0	0	+1
Spatial dimension	2	0	-1	-1
Ease of set up	2	0	-1	-2
Cost of production	3	0	-1	-1
Total score		**0**	**5**	**5**

The results from the Pugh chart show us that designs #2 and #3 are superior to our initial candidate design. The control system and enclosure of candidate #2 and #3 score more points over candidate #1. The drawbacks are their ease of setup being more difficult, and the large formats and complications make them difficult to configure and maintain. The only design that regulates the ambient temperature around the part is design #3 without having to print extra material. The same mode can be controlled with multiple heating elements better than an ambient bed we found later. In doing so the best of each design was evaluated and we decided on the best design as a meld of our most successful design components.

After evaluating the Pugh chart, we decided that a combination of the candidate designs could better accomplish the stakeholder requirements and engineering specifications. This new final design would include a printing enclosure, heating elements surrounding the bed, an ABS adhesive, a control system to regulate the bed and ambient temperature, and a vent fan for ABS exhaust fumes. This can be seen in Figure 11. Combining these components allows us to fully control both the gradient of the plate and the ambient temperature. We do this by regulating the ambient by exhausting the hot fumes when and heating the air with a coil surrounding the plate. This perimeter heating element can control both the regulatory heating control system and regulating exhaust fan that also expels noxious ABS fumes.

An enclosure allows for the regulation of the enclosed temperature and allows us to control the volume of the vapor surrounding the printing bed. We will also keep in mind to store the feed polymer and power supply outside the enclosure so they do not adversely affect printing. After performing some modeling, heating elements surrounding the perimeter of the bed were thought to be the best solution to maintain the build plate at a more uniform temperature as shown in Figure 12. This idea will create a temperature gradient that can be easily monitored in connection with the main heating element already present in the Ender 3. Similarly, this can help raise the temperature in the ambient air.

The ABS adhesive allows us to best ground the part when the print is at its most vulnerable and critical stage at the beginning of the print. The vacuum system, while interesting, was deemed

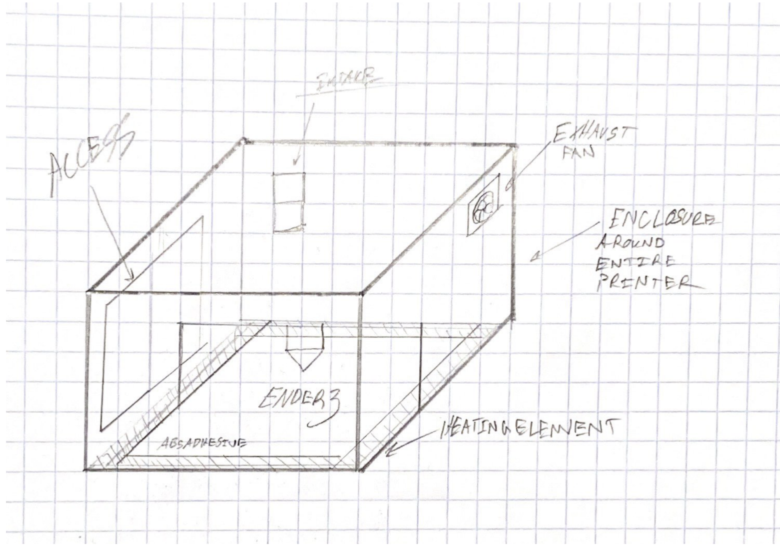

Figure 11: Sketch of Final Design Concept.

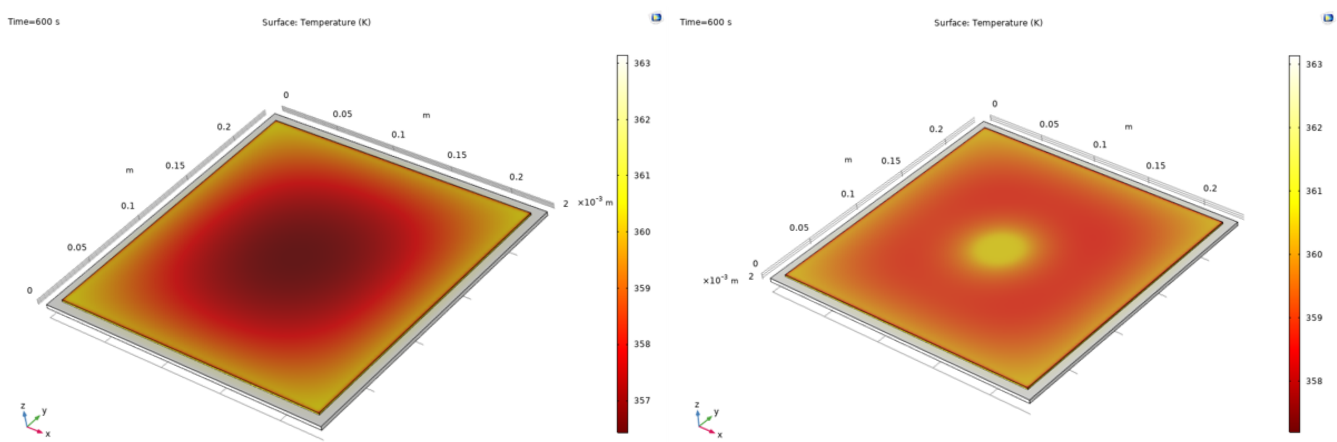

(a) Heat Source: Edge.

(b) Heat Source: Edge and Center.

Figure 12: COMSOL Thermal Models of Heating Elements Placement on the Printing Bed.

to be too high-risk and expensive for our purposes. We reasoned that considering the extensive modifications the perforated bed and vacuum system would require, if it was not as effective as anticipated or was implemented incorrectly in the testing phase, we would easily exceed our budget and run out of time. We determined that other solutions would be more effective and present lower risks. In order to have the most control over the ambient and bed temperature, a control system would be the best option. Finally, a vent fan would expel the ABS exhaust fumes that would otherwise be controlled in the enclosure. It would also be possible to use this fan to regulate the temperature if the bed needs to be heated in the case that the ambient temperature is already too hot.

3 Solution Development and Verification

3.1 Engineering Analysis

3.1.1 Concept Re-evaluation

After the concept selection phase of our design process, we met with our project sponsor Prof. Okwudire to get his input on our selected design, and he provided some insightful feedback. First, the idea of creating a temperature-controlled enclosure has been explored in the past and may not apply to our Ender 3 printer for various reasons. The first reason is that the cost of constructing such an enclosure is likely to significantly increase the cost of our solution. Since the Ender 3 printers are designed to be budget-friendly, it seems counter-intuitive to expect the Ender 3 users to purchase expensive secondary products to improve its print quality. Second, the Ender 3 printer may not be able to operate in a high-temperature environment. Some components, such as the belts, plastic guide rails, and wires, may deform when exposed to high temperature for a prolonged period. This can potentially worsen the quality of the printed parts. Even more problematic, our printer can break down and cause safety hazard. Weighting the viability of our solution, Prof. Okwudire recommended us to focus on controlling the temperature of the build plate. Temperature variation on the build plate has proven to be one of the causes of warpage and other thermal-induced defects in 3D printed parts. Hence, a solution to improve temperature uniformity on the build plate is valuable for our stakeholders.

This discussion had led us to develop a new phased approach to our solution to help avoid any unnecessary complexity. We divided our chosen solution concept into three distinct phases, as seen in Figure 13. The first phase consists of three elements labeled Phase 1.1, 1.2, and 1.3, respectively: a build plate control system with conduction heating elements, an enclosure made from construction-grade insulation, and an ABS adhesive. We would then conduct testing on this solution. During Checkpoint 1, if the ambient temperature in the enclosure surpassed 40°C, then we need not to move to Phase 2. However, if it does not achieve this value, moving on to Phase 2 is justified. This will be justified in subsequent analysis. Phase 2 includes the addition of a separate control system using convection to control the ambient temperature inside the enclosure. After developing the solution to this point, we would then evaluate where we stand. If time and budget allow us, we can move into more complex subsystems in Phase 3. Phase 3 would include the installation of a venting system to dissipate heat as necessary from the enclosure and control humidity. We may also change our enclosure material to Plexiglass with reflective interiors in this stage to prevent radiation heat transfer.

3.1.2 Solution Construction

To begin solution development, a high fidelity CAD model is constructed. The enclosure is modeled in cyan and is transparent for the purposed of noting its size in comparison to the Ender 3 printer. Additionally, the four heating elements are shown in magenta and are located in the middle of each side of the build plate. The model can be seen in Figure 14.

The first step of constructing our solution is attaching the heating elements. As will be justified below, it is most beneficial to place the heating elements along the bottom of the aluminum plate of the printer (which lies underneath the polyetherimide plate) and near the four cardinal edges. This is the same layer in which the Ender 3 houses its heating element and sensor; this heating element uses resistive heating to heat the entire bed with limited control. The four temperature control module sensors were also placed underneath the plate near the edges and the thermistors.

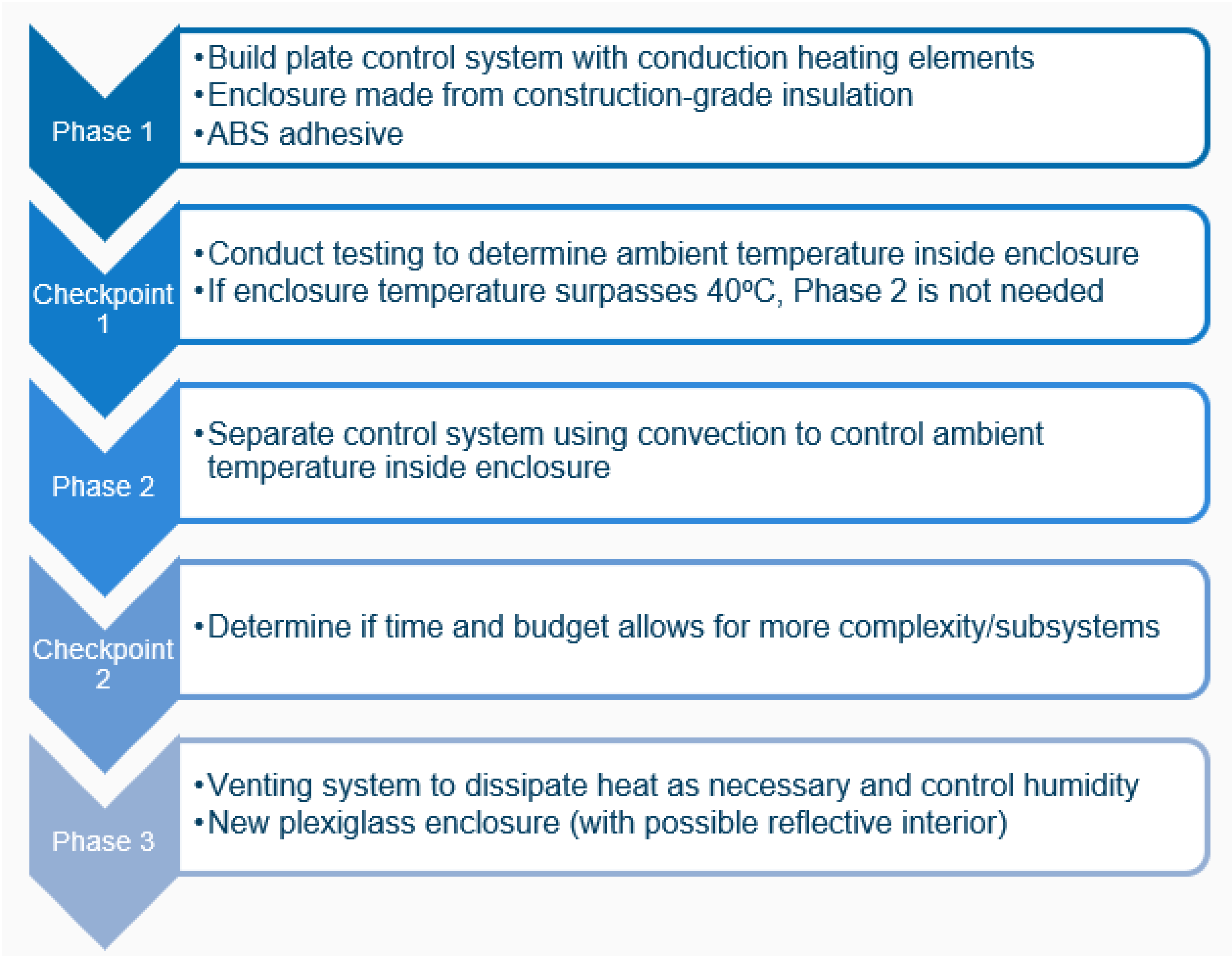

Figure 13: Phase approach design diagram.

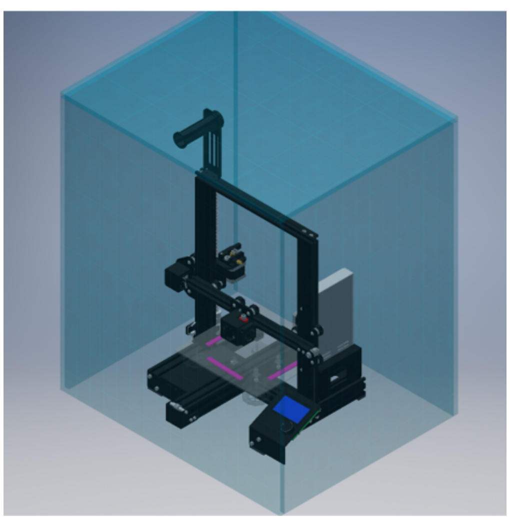

(a) Printer in cyan enclosure (enclosure transparent for model).

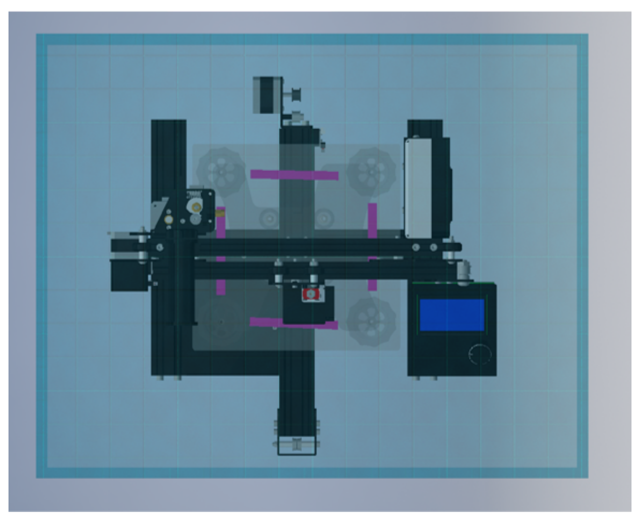

(b) Additional Copper Plate Model.

Figure 14: Heating element (magenta) location on print bed.

Nine thermistors measure the temperature in all nine regions of the build plate. The setup can be seen in Figure 15.

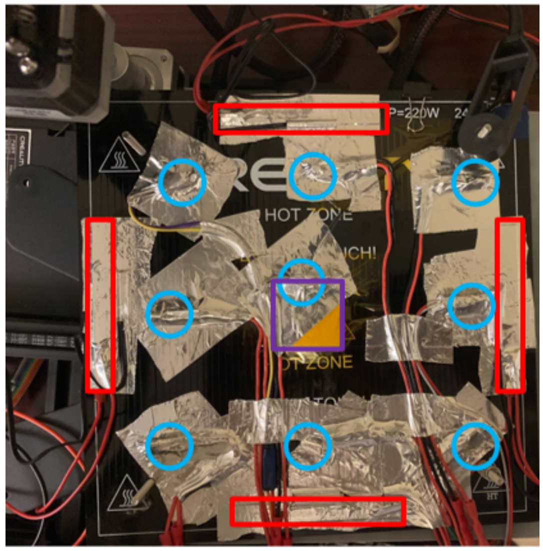

Figure 15: Underside of the heating bed (aluminum plate). Heating elements (red rectangle), thermistors (blue circle), and the Ender's thermistor (purple square) indicated.

3.1.3 Phase 1.1: Build Plate Conduction Control System

Before advancing to solution development for this phase, we returned to the build plate temperature experiment we performed earlier in the semester. We tested the Ender 3's capability to reach a set temperature of 90°C. We let the bed reach a steady-state value based on the temperature setting and observed the temperature variation on the build plate. Several changes are made since the aforementioned experiment. First, we refined our data acquisition system and re-calibrated the system. Second, we replaced a thermistor that produced a significant amount of noise in the last experiment. Finally, we performed the same experiment with our new enclosure, whose details are presented below in Phase 1.2. The result of the new build plate temperature experiment is presented in Figure 16.

We can see from Figure 16 that most of the regions are close to the set temperature of 90°C. However, two regions' temperature readings are above the set value (Regions 3 and 6), and two regions' temperature readings are below this set value (Regions 2 and 4). The low temperature in Region 4, the center region, can be explained by the position of the thermistor. Typically, the thermistors are attached to the bottom side of the heating element. However, in Region 4, there is a temperature sensor native to the Ender 3's control system, as seen in Figure 15. We cannot attach a thermistor directly to the build plate in this region and have to attach it to the sensor. This added thermal resistance creates a lower temperature. We are not concerned about the temperature in this region because the Ender 3's control system can regulate Region 4's temperature most closely since the sensor is attached directly under the region. Furthermore, we also know from our stakeholders that quality issues generally don't occur in the center of the build plate. On the other hand, region 2's low temperature is a concern to us and our stakeholders and motivates our solution.

We repeat the build plate temperature experiments multiple times, and we find that the temperature distribution varies between experiments. As a result, we cannot reliably predict the underheated regions or target those regions effectively. Such a phenomenon is likely caused by the Ender3

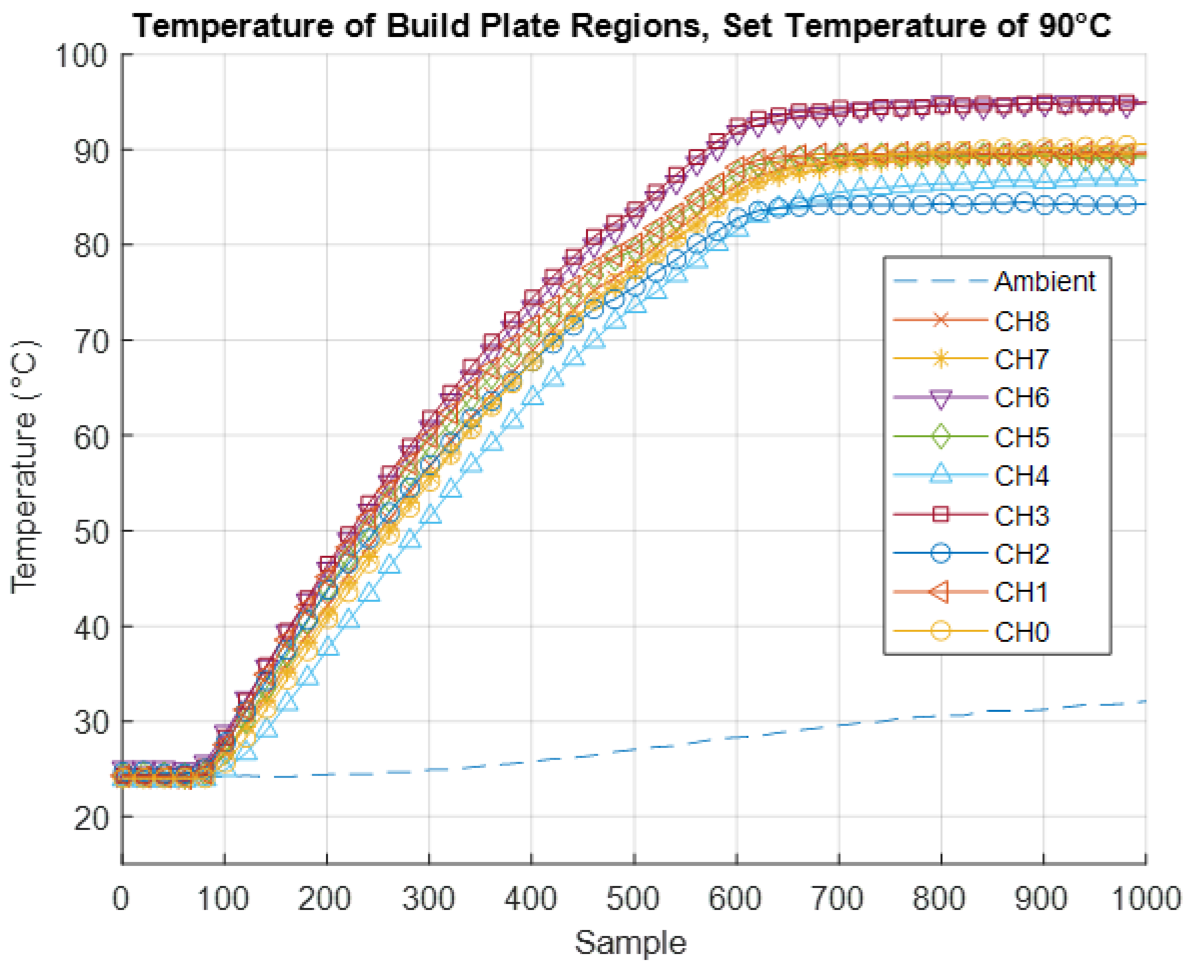

Figure 16: Steady state temperature values of the various nine build plate temperature regions with an enclosure (where CH refers to the data acquisition channel at each of the 9 regions).

build plate temperature control system. Even though the Ender3's resistive heating elements cover the entirety of the build plate, uniform heating is not guaranteed. The resistance value of the heating elements is flexible to small changes, which can then lead to a noticeable difference in heat dissipation. Additionally, the Ender 3's temperature control system relies only on one thermal sensor that measures the temperature at the center of the build plate, and hence temperature in other regions are not well-regulated.

Since we know that the existing Ender 3 heating element heats the center well but struggles to reliably heat other regions, we modeled the current state in an exaggerated fashion in COMSOL in Figure 17a. This COMSOL model represents the Ender 3's heating element as a heat source at the center of the build plate where its sensor is located. We then explored different heating configurations for our heating elements, and we found that the configuration in Figure 17b provided the minimum temperature gradient across the build plate. This configuration uses heating elements on the edges of each side of the build plate. This is our selected heating element design with four heating elements in this configuration.

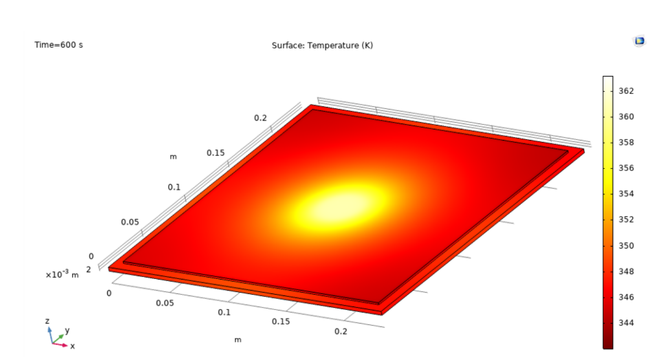

(a) Temperature distribution on build plate given center source.

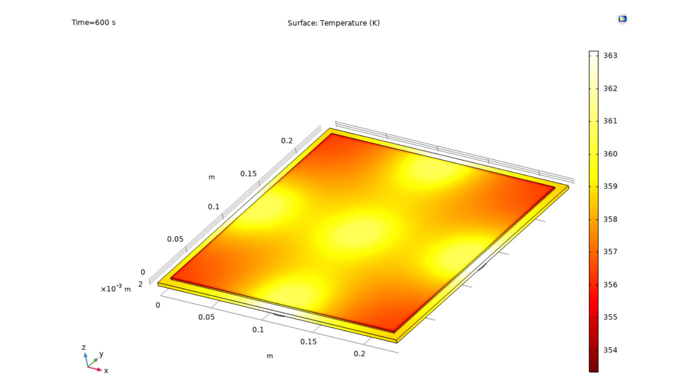

(b) Temperature distribution on build plate given edge source.

Figure 17: COMSOL Heating Models.

3.1.4 Phase 1.2: Enclosure

The next step in constructing our solution is to create the enclosure. We want a material that has a low cost, functions as a good insulator that can help maintain the ambient temperature in the enclosure, and is readily available in stores (due to COVID-related delivery issues). As a result, we decide to use polystyrene foam. The thermal conductivity of the foam is approximately 0.024 $\frac{W}{m \cdot K}$, which indicates good thermal insulating capability. The enclosure is a rectangular cuboid with one of the faces being the surface on which the 3D printer is placed on. The foam is $\frac{1}{2}$ inches thick with the dimensions of $480 \times 600 \times 720$mm. The physical prototype of the enclosure is shown in Figure 18.

Figure 18: Physical prototype of the enclosure

The enclosure will retain a lot of heat given the high ambient temperature inside, and this raises safety concerns with its handling. We do not want an operator to interact with the enclosure if the outside surface of it is too hot. However, it is also not ideal to ask the operators to wait for a long time for the enclosure to cool down. We perform a thermal circuit analysis to understand how the ambient temperature inside the enclosure affects the surface temperature of the enclosure.

The schematic of the thermal circuit is shown in Figure 19. The detailed calculation is shown in Appendix D.

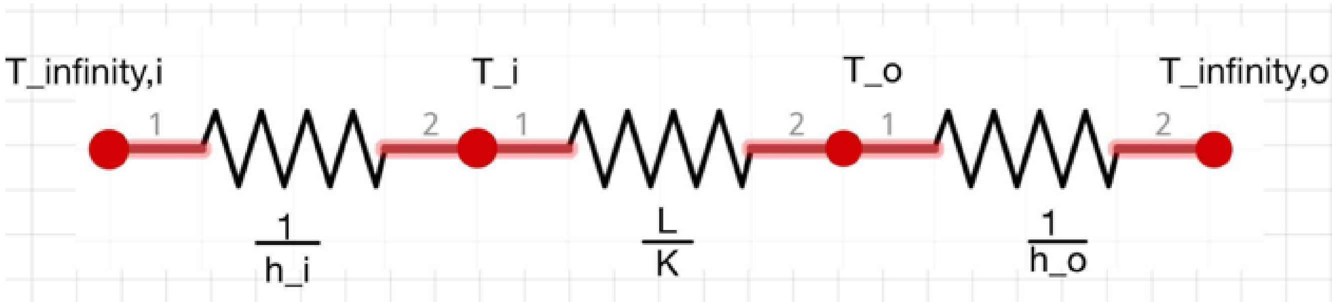

Figure 19: Thermal circuit analysis performed on the enclosure to gauge the outside temperature of the enclosure.

To perform the analysis, we need to choose the ambient temperature inside the enclosure ($T_{infinity,i}$). Using data from previous build plate temperature experiments, we choose a value of 40°C. After performing the analysis, we find that the surface temperature can reach up to 25.495°C. This temperature is deemed safe for humans to handle, given the fact that this temperature is not much hotter than most room temperature of 23°C.

3.1.5 Phase 1.3: ABS Adhesive

After evaluating various types of adhesives to use with the printed ABS we concluded using a polyetherimide (PEI) plate. The plate will be used instead of the polycarbonate plate already installed on the 3D printer. The other candidates included ABS juice, Kapton tape, and regular glue.

ABS juice is a mixture of acetone and ABS with a predefined ratio. It is usually prepared and applied to to the build plate right before the print. ABS juice is widely utilized in the hobbyist community due to its low cost, readily available stock materials, and good adhesion, according to one of our stakeholders. However, it was found that this may be too cumbersome for a user to make and apply before every print in our solution. There are also concerns with a user making the mixture incorrectly which could result in negative effects in the print and potential safety hazards for the user.

The Kapton tape is another popular alternative. It provides good adhesion and facilitates easy removal of printed parts from the build plate [10]. The downside of Kapton tape is that a large Kapton tape sheet is significantly more expensive than other alternatives, and it has to be reapplied after a few prints. As a result, using Kapton tape is not budget-friendly and can be unnecessarily laborious for users to apply.

The final alternative was glue. This solution is known to work to a lesser degree and can result in very messy aftermaths. Unfortunately, there is no quantitative way to compare the solutions without testing due to limited time and budget. The PEI plate can be seen on our Ender 3 in Figure 20.

3.1.6 Control System Modeling

In this section, we present the modeling of the control system. First, we introduce the objective and assumptions involved in the modeling process. Then we show the modeling of the plant and

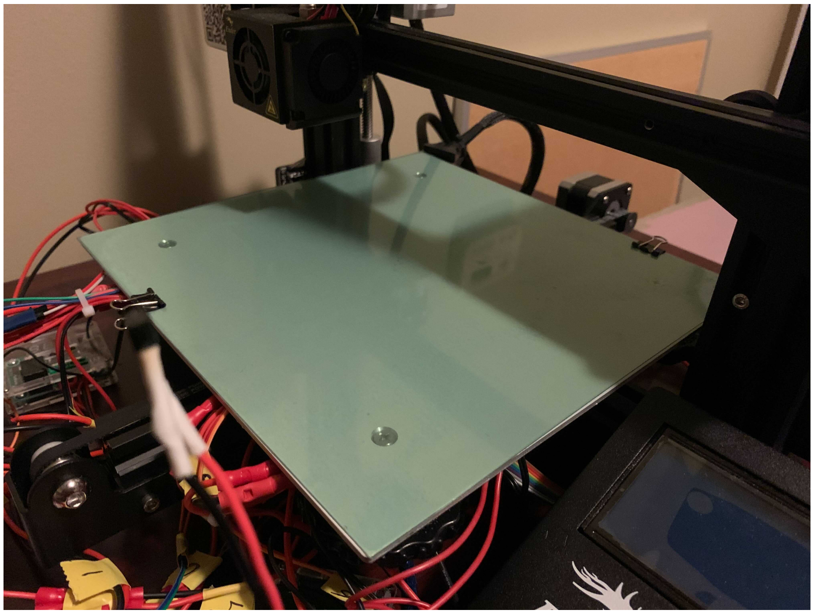

Figure 20: Polyetherimide plate placed on the aluminium printing bed for better ABS adhesion.

the closed-loop control system. Finally, we present the selection of the controller for the control system.

3.1.6.1 Objective and Assumptions

The objective of creating a model and perform control is to achieve uniform temperature across the build plate. Uniform build plate temperature is important because it is critical in reducing warping in 3D printed parts [8]. However, to achieve a high degree of temperature uniformity, we need to determine the temperature gradient of the build plate, and this requires sophisticated measurement tools, such as infrared cameras. Given the constraints on the budget, we use thermistors to obtain temperature at certain points on the build plate. The first assumption is that *the temperature at the centers of the nine regions, shown below in Figure 21, can reasonably represent the temperature of that region.*

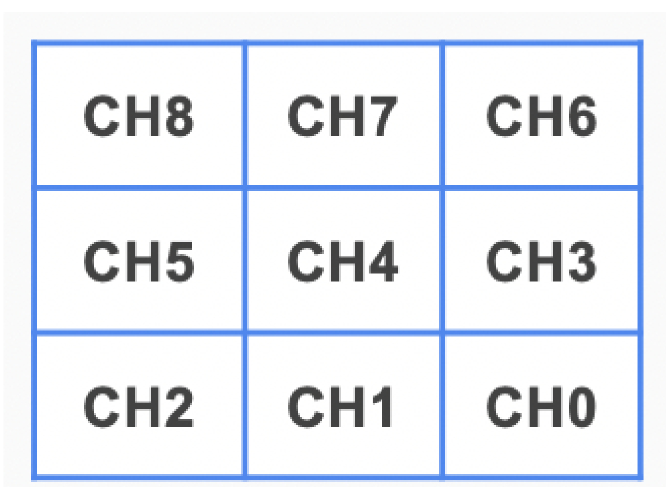

Figure 21: Build plate region schematic.

We conducted experiments to determine the temperature variation across the nine regions, and we found that some regions are significantly colder than in other regions. As a result, we aim to regulate the temperature at the regions that is colder than the set build plate temperature. Due to spatial constraints, we are only able to position four heating elements under the build plate. We make the second assumptions that *each heating element is capable of regulating the temperature of a* $23' \times 7.2'$ *region.*

3.1.6.2 Closed Loop Control System

The system consists of the build plate and the four heating elements. Since each heating element can receive a reference, and we can measure the temperature around each heating element, the system has four inputs and four outputs. To determine how each input related to each input, we performed an experiment where we turned on one heating element and monitored the temperature around the neighboring two heating elements. The experimental data is shown in Figure 22, and we can conclude from the experimental data that the heating element does not affect the temperature around neighboring heating elements. As a result, we can model the system as four single input single output systems, and each system has one reference input and one temperature output.

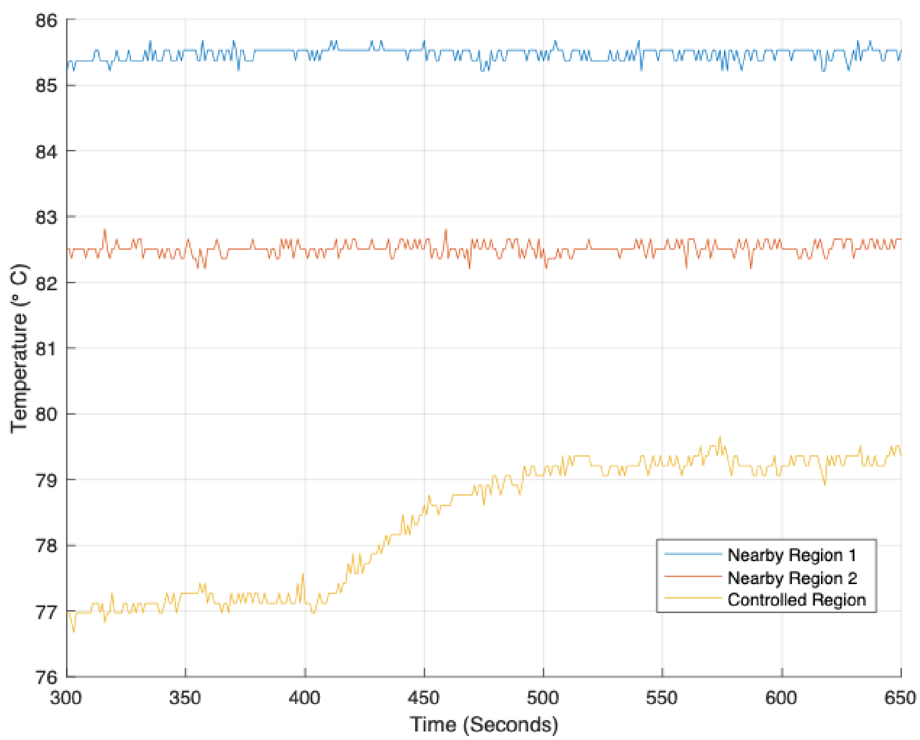

Figure 22: Heating element effects on neighboring regions.

Using experimental data, we determined that each system can be modeled as a first-order system, and the first-order system is governed by the following differential equation

$$m\dot{T} + cT = f \tag{5}$$

where T is the temperature of the build plate, f is the step forcing function, and c, m are the constants that describe the system. The solution of the differential equation is in the form

$$T(t) = T(0)e^{-\frac{ct}{m}} + \frac{F}{c}(1 - e^{-\frac{ct}{m}}) \tag{6}$$

where F is the magnitude of the step forcing function f. We can determine the constants c, m by solving the following two equations

$$T(\infty) = \frac{F}{c} \tag{7}$$

$$T(t_i) = T(0)e^{-\frac{ct_i}{m}} + \frac{F}{c}(1 - e^{-\frac{ct_i}{m}}) \tag{8}$$

We solved equation (7) and (8) above and obtained $m = 45.5$ and $c = 1$. The system has a time constant of 45.5 seconds.

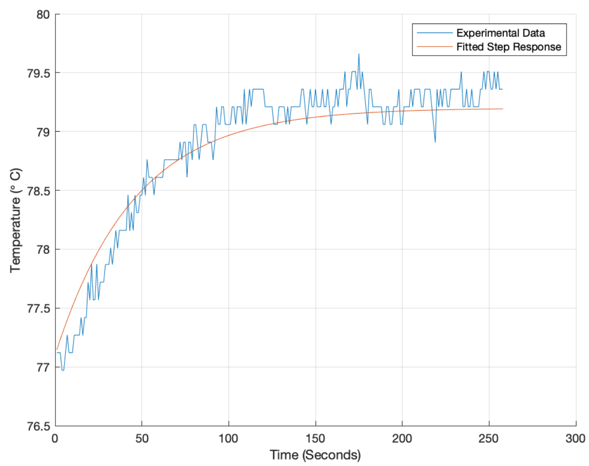

Figure 23: Fitted step response of system and experimental data.

To control the system, we construct a closed-loop control system, and the block diagram is given in Figure 24. We decided to use the W1209 temperature control module as our controller because of its low cost, built-in temperature sensor, and ease of use with both high and low power electronics.

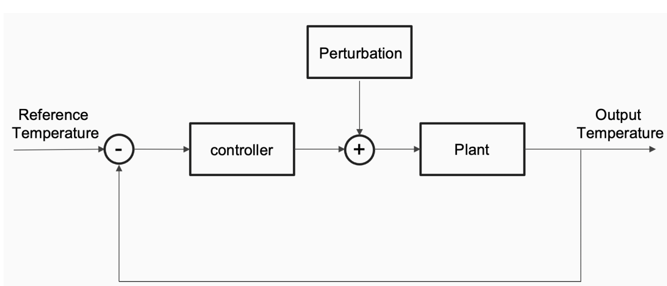

Figure 24: Closed loop control system block diagram.

3.1.7 Enclosure Temperature Analysis

To gain a better understanding of the heat transfer phenomenon in the system we created a simple heat transfer model. In this model, we look to evaluate the one-dimensional temperature gradient in the y-direction of a rectangular block with a square cross-section (dimensions 3cm × 3cm × 5cm) from its base to its height. In this model, we assume that the only forms of heat transfer are one-dimensional conduction throughout the part and convection heat transfer with the ambient air on the four rectangular surfaces. We also make the assumptions regarding the boundary condition with a temperature of $T(y = 0) = 90°C$ (a constant temperature on the printing bed when printing ABS) and a temperature of $T(y = 0.05) = 240°C$ (temperature of the polymer after immediately being extruded). This analysis will be completed using a control volume analysis. The model and control volume for this analysis can be seen in Figure 25. The governing equations for this model will be Fourier's law of conduction, Newton's law of cooling, and the conservation of energy.

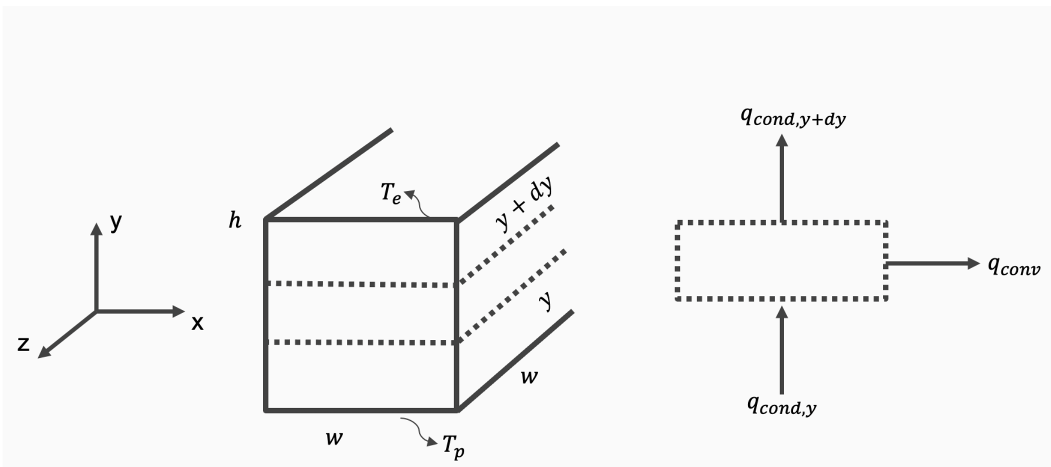

Figure 25: Model and control volume used for analysis.

We can begin this analysis by writing Fourier's law of conduction for the infinitesimally small control volume with a height of y as seen in the Figure above which yields Equation (9).

$$q_{cond,y} = -kA\frac{\partial T}{\partial y} = -kw^2\frac{\partial T}{\partial y} \tag{9}$$

where $q_{cond,y}$ is the heat transfer when y = y, k is the thermal conductivity of the part, A is the cross-sectional area, w is the side of the square cross-section, and $\frac{\partial T}{\partial y}$ is the partial derivative of temperature with respect to the spatial dimension y. Taking the partial derivative of Equation (9) leads to Equation (10).

$$\frac{\partial q_{cond,y}}{\partial y} = kw^2\frac{\partial^2 T}{\partial y^2} \tag{10}$$

We then find the conduction equation for the infinitesimally small control volume when y = y + ∂y by using the Taylor series expansion and ignoring higher terms. The result is seen in Equation (11).

$$q_{cond,y+dy} = q_{cond,y} + \frac{\partial q_{cond,y}}{\partial y}\partial y \tag{11}$$

We know that Newton's law of cooling acts on the control volume as seen in the figure above and reduces to Equation (12).

$$q_{conv} = hA(T - T_\infty) = h(4wdy)(T - T_\infty) \tag{12}$$

where q_{conv} is the convection heat transfer coefficient, A is the surface area affected by convection, w is the side of the square cross-section, dy is the infinitesimally small height of the control volume, T is the temperature of the surface, and T_∞. We can then use the conservation of energy for the control volume. We assume steady-state conditions and no energy generation inside the control volume. This expression is given in Equation (13).

$$\cancelto{0}{\dot{E}_{cv}} = \dot{E}_{in} - \dot{E}_{out} + \cancelto{0}{\dot{E}_g} \tag{13}$$

where $\dot{E}_{cv}$ is the rate of energy storage in the control volume, $\dot{E}_{in}$ is the rate of energy entering the control volume, $\dot{E}_{out}$ is the rate of energy leaving the control volume, and $\dot{E}_G$ is the rate of energy in the control volume. We can then substitute the forms of energy entering and exiting the control volume from our figure which leads to equation (14).

$$0 = q_{cond,y} - q_{cond,y+dy} - q_{conv} \tag{14}$$

Substituting Equation (11) into Equation (14) will yield Equation (15).

$$0 = q_{cond,y} - (q_{cond,y} + \frac{dq_{cond,y}}{dy}dy) - q_{conv} \tag{15}$$

Performing arithmetic in this equation will give the result in Equation (16).

$$\frac{dq_{cond,y}}{dy}dy = q_{conv} \tag{16}$$

We can then plug in Equations (10) and (12) into Equation (16) to give the result in Equation (17).

$$-kw^2\frac{\partial^2 T}{\partial y^2}dy = h(4wdy)(T - T_\infty) \tag{17}$$

Rearranging and manipulating Equation (17) will give us a more practical form in Equation (18)

$$-kw\frac{\partial^2 T}{\partial y^2} + \frac{4h}{kw}(T - T_\infty) = 0 \tag{18}$$

We can then make a useful substitution that will help us get Equation (10) into a better form to solve. Let $\theta = T - T_\infty$, such that $\frac{\partial\theta}{\partial y} = \frac{\partial T}{\partial y}$ and $\frac{\partial^2\theta}{\partial y^2} = \frac{\partial^2 T}{\partial y^2}$. Also, we can let $m^2 = \frac{4h}{kw}$. Making these appropriate substitutions into Equation (18) will gives us the canonical form seen in Equation (19).

$$\frac{\partial^2\theta}{\partial y^2} + m^2\theta = 0; \tag{19}$$

The well known general solution to this type of differential equation is given in Equation (20).

$$\theta(y) = c_1 e^{my} + c_2 e^{-my} \tag{20}$$

where c_1 and c_2 are unknown constants.The first boundary condition of our problem is shown again in (21) along with the substituted form using θ.

$$T(y=0) = T_p, \theta(y=0) = T_p - T_\infty \tag{21}$$

where T_p is the temperature of the heated build plate, and T_∞ is the temperature of the ambient air. Plugging the boundary condition in (21) into Equation (20) yields Equation (22) and simplifying that will give Equation (23).

$$T_p - T_\infty = c_1(1) + c_2(1) \tag{22}$$

$$c_1 + c_2 = T_p - T_\infty \tag{23}$$

The second boundary condition of our problem is shown again in Equation (24) along with the substituted form using θ.

$$T(y=h) = T_e, \theta(y=h) = T_e - T_\infty \tag{24}$$

where T_e is the temperature of the polymer right after being extruded, and T_∞ is the temperature of the ambient air. Plugging the boundary condition in Equation (24) into Equation (20) yields Equation (25).

$$T_e - T_\infty = c_1 e^{mh} + c_2 e^{-mh} \tag{25}$$

We then used MATLAB to solve the system of equations for the constants presented in Equations (23) and (25). The solution for the constants are presented in equations (26) and (27).

$$c_1 = \frac{T_\infty - T_p + T_e e^{mh} - T_\infty e^{mh}}{e^{2mh} - 1} \tag{26}$$

$$c_2 = \frac{-e^{mh}(T_e - T_\infty + T_\infty e^{mh} - T_p e^{mh})}{e^{2mh} - 1} \tag{27}$$

We can finally write the solution for the one-dimensional temperature gradient in the form of equation (28). This solution was graphed in MATLAB and is presented in Figure 26.

$$\theta(y) = T(y) - T_\infty = c_1 e^{my} + c_1 e^{-my} \tag{28}$$

Using the above analysis we performed another calculation. In the above case, we can see that the lowest temperature across the part occurred in an area above the build plate. If we change the ambient temperature in the analysis we can vary the minimum temperature in the part as a function of the ambient temperature. This process was done with an algorithm in MATLAB and the result is shown in Figure 27.

We can see from Figure 27 that the minimum temperature of the part increases as the ambient temperature increases. As the minimum temperature of the part increases the overall temperature gradient of the part decreases. To balance the heat tolerance of the parts of the Ender 3 and the desire for temperature uniformity, we want a target enclosure temperature of 40-60°C (313-333K). From this conclusion, we looked at previous data to see what the ambient temperature was approaching. From past experiments, we ran the printer to determine the steady-state values of temperatures in the 9 various regions which took approximately 18 minutes. However, we also had data for the ambient temperature with the enclosure on. This data can be seen in Figure 28. It was found that after 18 minutes, that the enclosure temperature reached approximately 35.6°C (with

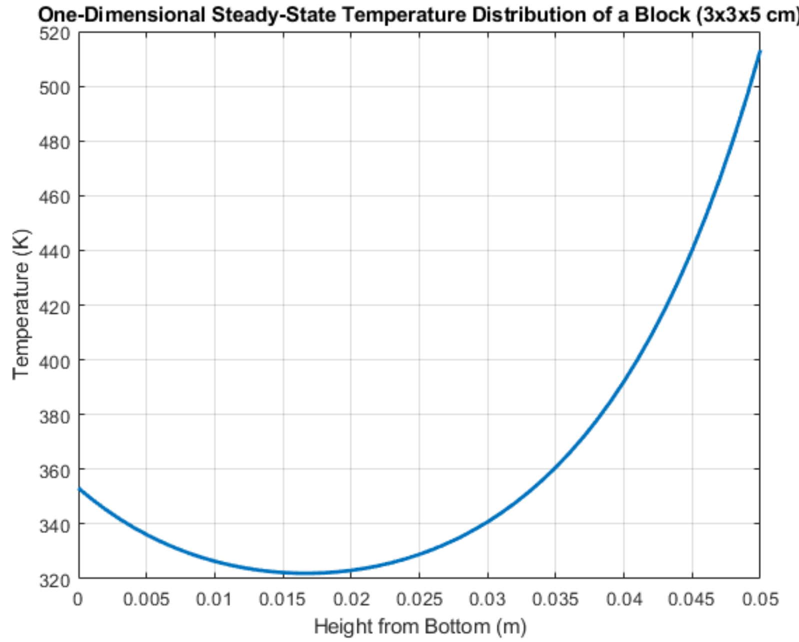

Figure 26: The variables used are: width = 3cm, height = 5cm, h = 10 W/m^2K, T_e = 240°C (513.15 K), T_p = 80°C (353.15 K), T_∞ = 20°C (293.15 K).

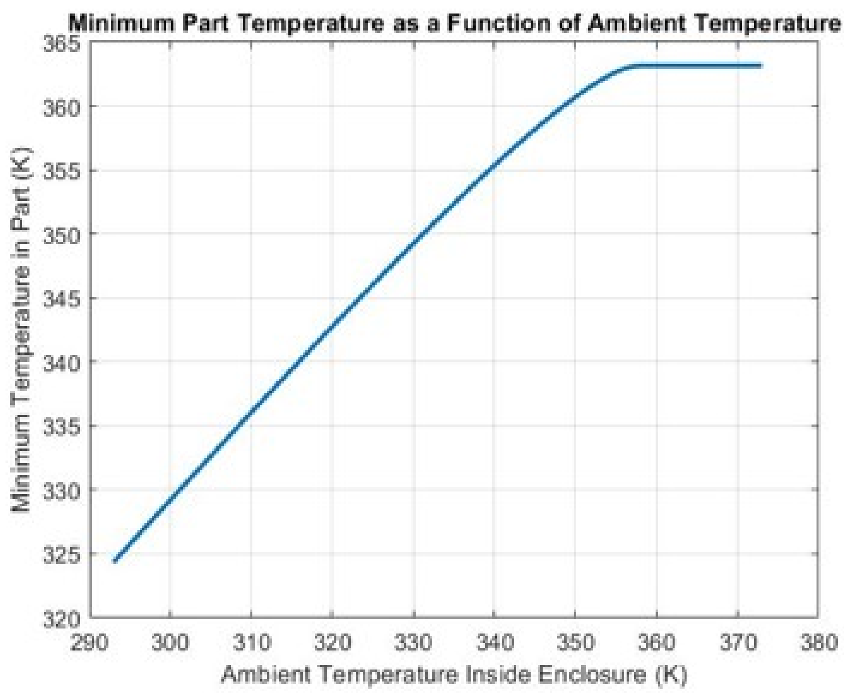

Figure 27: Minimum part temperature modeling.

the outside ambient temperature of the room at 21°C). The graph does not show signs of plateauing yet and as a result, we can confirm that the steady-state of the ambient temperature will approach the wanted range of 40-60°C given enough time.

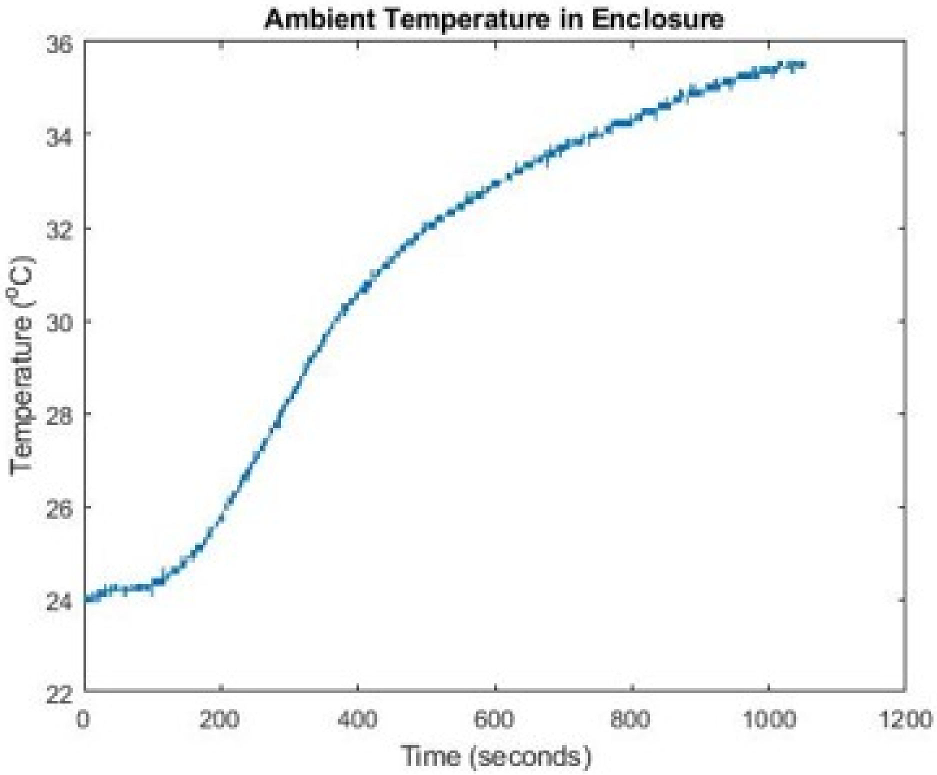

Figure 28: Ambient temperature inside the enclosure.

3.1.8 Transient Heat Transfer Analysis

In addition to the one-dimensional steady-state models we developed in COMSOL and by hand, we wanted to create a heat transfer model under transient conditions whose volume would change with time as the part is printed. We were able to develop a governing partial differential equation and an expression for how the volume changes as a function of time given the 3D printer's parameters. After meeting with Prof. Katsuo Kurabayashi, we learned more about the moving boundary condition and were able to develop expressions for the initial and boundary conditions. However, due to our unfamiliarity with partial differential equations, we are not able to solve them analytically or numerically using software such as Mathematica and MatLab. For the detailed derivation of the model, please see Appendix E.

3.2 Risk Assessment

For our project, we had completed a formalized risk assessment in the form of an early design Failure Mode and Effects Analysis (FMEA). The entire FMEA can be seen in Appendix L. From this analysis, we have determined that the greatest risks in our design fall under two categories. The first is thermal related effects and the second is electronics. Our system deals with a lot of high temperatures and as a result, there are concerns with getting burned or something catching on fire. Similarly, our system has a lot of electronic components that are connected with wires. This allows for hazards such as electrical shock or short-circuiting of components.

After reviewing our FMEA, we see that the occurrence of any of the failure modes are all fairly low. As a result, we do not believe that the system has a high chance of reaching any of the described failure modes. Our final system is not very complicated and has no moving parts. As a result, a lot of the occurrence of a failure mode has to do with the negligence of a user or a damaged material. The aspect of our design with the highest risk was the user experiencing electric shock due to wire issues. There are a lot of wires found throughout our solution and they can get entangled. If any parts of the wires were exposed or broken, the user may experience an electrical shock. We think the likelihood of failure would be very low as one normally does not touch electrical components, especially wires, during operation. We believe this failure has the highest risk associated with it because its severity is so high. As mentioned, we believe the occurrence to be rare, and detection should be rather high. If one were to touch wires at any point, we believe that one would ensure the power is off or to observe the wires to check for damages before any interaction. We did not make any design changes based on the risk of this design as wired connections are a vital part of our solution. From the FMEA, we also did not make any design changes. The associated risk with a lot of the components is fairly low and again, most are due to negligence or flawed parts. Overall, our solution is fairly simple with few components and we determined that the risk associated with it was low and acceptable.

3.3 Verification

In this section, we evaluate our solution and determine whether all the specifications are met. Additionally, we provide statistics to quantify the improvement generated from our solution from a warpage reduction and consistency standpoint. For simplicity, we refer to the experiment performed with our solution as the *final testing*, and the experiment performed without our solution as the *initial testing*. We use a standard test part for both testing experiments, and the test part's engineering drawing is shown in Figure 29.

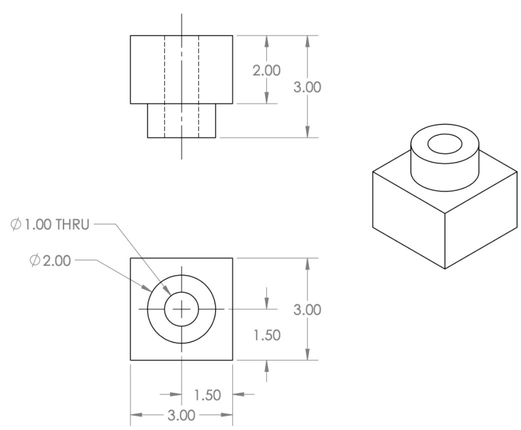

Figure 29: Standard Test Part CAD (dimensions in cm).

3.3.1 Final Testing

To evaluate the effectiveness of our solution and determine whether our solution meets the specifications related to warpage, we performed the final testing. We used the test part geometry shown in Figure 29 for a few reasons. First, it provided a wide range of features that could thoroughly test the capability of our solution against the initial state. When we intended at the beginning of the semester to use the CMM to measure many different features, the cylindrical and rectangular features provided an opportunity to do just that. We also designed the dimensions of the base to control how much warping we wanted to observe in the test part. In our initial trials, before we established the test part, we used a thinner geometry with a wider cross-section. This part warped significantly; its smallest corner height was just over half the height of the design height. To replicate the type of performance that our stakeholders might be experiencing, we chose a geometry that warped a little but not enough to routinely fail; this would not represent the current state properly. Combining this consideration and our literature review in designing test parts [16] [17] [18], we decided on a 2cm by 2cm square thick base as shown in Figure 29

To generate sufficient data for statistical analysis, we performed three sets of identical experiments. To provide sufficient comparison with our initial testing, each experiment is conducted three times with and without our solution – insulation enclosure and build plate temperature control system – in place. For both the initial and final testing, nine parts were printed at a time. One part was printed in each region as labeled in Figure 21.

Due to difficulty in accessing testing equipment such as a coordinate measurement machine and a profilometer, we only used corner height measurements of the printed test parts to evaluate the effectiveness of our solution in reducing warpage and improving consistency among printed parts. The height of each corner is measured four times and the average value is recorded. In total, we generated $3 \cdot 9 \cdot 4 = 108$ data points of corner height for both the initial and final testing. The mean and standard deviation of corner height measurements are provided below in Table 4. The mean measures the overall dimensional accuracy of the parts, and the standard deviation measures the degree to which individual corner height deviates from the mean. Our solution does not provide a meaningful improvement in terms of dimensional accuracy, and this is expected because our solution is not designed to counter shrinkage in 3D printing. On the other hand, our solution markedly reduces the standard deviation, and this indicates that our solution improves the dimensional consistency of the printed parts. The final and initial testing data are also used to compute metrics that determine whether our solution satisfy the engineering specifications we outlined in the problem definition phase.

Table 4: Mean and standard deviation of final and initial testing.

	Mean	Standard Deviation
Final Testing	19.297 mm	0.215 mm
Initial Testing	19.029 mm	0.846 mm
Percent Improvement	1.407%	74.552%

3.3.2 Specification 1: Warpage Prevention

The specification requires that the dimension at each corner of the test part should not deviate more than 20% from the median corner dimension of the test batch. We refer to this metric as percent deviation from median corner height, and it is defined as follows.

$$\text{Percent Deviation from Median Corner Height} = \frac{|h_{ik}^{j} - m^k|}{m^k} \tag{29}$$

h_i^j is the height measurement of the j^{th} corner of the i_{th} test part in the k^{th} batch.

All 108 measurements from final testing and all 108 measurements from the initial testing satisfy this specification. The fact that all the initial and final test parts passed points to the fact that a 20% metric is a conservative one for our test part. From our stakeholder interviews, we learned that 3D printed parts often have tolerances of "as printed." This means that these are not high tolerance parts, and unless there is excessive warping, they are still functional. Our team turned these observations and our experience into a metric of 20%, denoting the maximum warping allowed for an "as printed" part. Given that this was a minimum specification and that we selected a test part that would not warp excessively, this very high passing rate for all parts makes sense. Since we want to quantify the improvement created by our design, we lowered the 20% threshold to 1%. By tightening this specification, we are considering the desired specification, not just a minimum specification - one that would allow for tighter tolerance parts to be printed. Thus, we repeated the calculation of this requirement with the threshold set to 1%, and the final testing parts significantly outperformed the initial testing parts. 88 out of 108 measurements from the final testing deviated less than 1% from the batch median, compared to 47 out of 108 measurements from the initial testing. Thus, our passing rate increased from 43.519% to 81.481%, an 87.231% improvement.

Additionally, we calculated the average deviation of the final and initial testing parts. The average deviation of the final testing parts is 0.644 mm, and the average deviation of the initial testing parts is 2.380 mm. This marks a 72.932% percent in terms of warpage reduction.

3.3.3 Specification 2: Consistency

This specification requires that the standard deviation of the corner height measurements of a part be less than 5% of its mean corner height dimension. We refer to the metric used in this specification as a percent standard deviation of part corner height, and the metric is defined as follows.

$$\text{Percent Standard Deviation of Part Corner Height} = \frac{d^i}{\frac{1}{4}\sum_{j=1}^{4} h_{ik}^{j}} \tag{30}$$

d^i is the standard deviation of the corner height measurement of the i^{th} part, and h_i^j is the height measurement of the j^{th} corner of the i_{th} test part in the k^{th} batch.

All 27 printed parts from the final testing met this requirement, but only 24 out of 27 parts from the initial testing fulfilled this requirement. Using the same logic as in Specification 1, we repeated the calculation of this requirement with the threshold set to 1%. With this more aggressive threshold, our final testing parts again significantly outperformed the initial testing part. Only 11 out of 27 initial testing parts, or 40.741%, achieved a corner height standard deviation of below 1% mean corner height. On the other hand, 24 out of 27 final testing parts, or 88.889%, satisfied the 1% threshold, representing a percent improvement of 118.181%.

3.3.4 Specification 3: Quality

This specification requires that the first pass yield is above 90% for 3D printed parts. First pass yield is defined as follows:

$$\text{First Pass Yield (FPY)} = \frac{\text{Number of Qualified Parts}}{\text{Number of Produced Parts}} \tag{31}$$

A part is counted as qualified if none of its corner dimensions deviate from the design dimension for more than 7.5% percent. 26 out of 27 parts from the final testing are counted as qualified, and 17 out of 27 parts from the initial testing are counted as qualified. The final testing has a first pass yield of 96.296%, and the initial testing only achieved 62.963%. Our solution improves the first pass yield by 52.941% and meets the specification of 90%.

3.3.5 Specification 4: Cost Efficiency

Our cost-efficiency specification mandates that our solution must have a prototyping cost below \$200 and a production cost below \$90. As seen in our Bill of Materials in Appendix F, the cost of our prototyped solution was \$72.73, below the prototyping cost of \$200. If we even include the cost of development, including all of our costs except the cost of the printer and ABS filament, our cost still meets our specification at \$188.25. When considering our production cost, we consider our current unit cost and other potential costs. Our unit cost for materials is just \$72.73, although that does not include labor and overhead. However, if our solution was produced at scale, we would be able to source our components much more cheaply. Since our material costs are already below \$90 and it would be purely speculative to calculate labor and overhead costs, we determined that our cost of \$72.73 meets our specification of \$90.

3.3.6 Specification 5: Spatial

The specification requires that our solution does not extend the envelope of the printer more than 20% in the length and width dimension. The printer envelope and our solution (enclosure) dimension are listed in Table 5. Our solution (enclosure) extends the length direction by 5.660% and the width direction by 10.870%. As a result, our solution meets this specification and is space-efficient. Our industry stakeholders will not need to adjust their 3D printer layouts much to accommodate our solution if they have a few printers next to each other in a room.

Table 5: Printer envelop and enclosure dimension.

	Length	Width	Height
Enclosure Dimension	56	51	71
Printer Envelop Dimension	53	46	71

3.3.7 Specification 6: Ease of Setup

This specification requires the setup time of our solution to be under 60 minutes. Our team member, Luthfor, takes about 20 minutes to set up our solution. Assuming a safety factor of 2 to account for someone who isn't as skilled and isn't as familiar with our design, our solution can be assembled in about 40 minutes. This is less than 60 minutes, meaning we meet this ease of setup specification.

3.3.8 Summary of Design Solution Results

Our solution satisfies all of the engineering specifications. In particular, our solution reduces warping by 72.932% and improve of the printed parts consistency by 118.181%. By our definition of first pass yield, our design achieves 96.296%, an improvement of 52.941% over the initial case. Our design also meets the cost efficiency, spatial, and ease of setup requirements.

4 Discussion and Recommendations

4.1 Design Strengths and Successes

Having successfully constructed our prototype, we noticed that the system performed extremely well. We found a 72.932% percent decrease in part warping. We believe the system's enclosure did a very good job of trapping waste heat from the printer bed's heating source and our heating modules (around a constant 42°C). This kept the parts at a much higher uniform temperature than without the enclosure which we believed was a major contributor to the success. Also, the printing modules did a very good job of keeping the temperatures at a more uniform temperature. The maximum build plate temperature deviation in a single region was $10°C$ in our initial testing but $2°C$ in our final testing. This led to greatly increased consistency among the parts. Using the heat transfer analysis as well as the COMSOL heat modeling gave us insight into the build plate temperature problem as well as the heat transfer inside the parts. These analyses helped shape how we determined our final design as well as the level of control we could impart onto the system. We did this after DR2 but it would've been more helpful to do sooner to determine our path earlier on in the design phase.

Another main strength of our design was its lack of unnecessary complexity. In our concept exploration phase, we wanted our final solution to have an enclosure, a build plate control system, a convection control system, and venting system, and an adhesion solution. After Design Review 2, we received valuable feedback from our sponsor that led us to develop a phased approach. In Phase 1, we focused on the enclosure, build plate control system, and adhesion. We then conducted testing to see whether Phase 2 was needed in our solution. As explained previously, Phase 2 was unnecessary because the temperature inside the enclosure reached $40°C$. We decided that the venting system and a better enclosure would be saved for Phase 3 if time and budgeting allowed to make sure that the design worked first. This phased approach was very successful, creating a lean design that was very effective without introducing unnecessary subsystems. We were able to implement and rigorously test Phase 1 solutions, rule out the complexity and cost associated with Phase 2, and ready our design for future iterations that include Phase 3 solutions.

4.2 Design Weaknesses

While our design performed very well and was successful, it has some weaknesses as well. First, while this design passes our ease of setup specification, we think that significant improvements can be made in this area. Since our goal is to provide an industry 3D printing user with an easy kit to install, making users assemble the build plate control system themselves is not a good idea. This can be cumbersome for the end-user, especially one who does not have much experience with electronic equipment. Most low-cost 3D printers are turnkey products that require little modification and our current design is a departure from that.

The build plate control system and the heating elements, in particular, have weaknesses as well. In our testing, we found that our placement of the heating elements allows for maximum reach across the necessary cold regions without creating a complicated MIMO system in which the heating elements would influence each other. While this allows us to use a SISO model for our control system, the limited reach of the heating elements can be a challenge for printers that have greater build plate temperature variations.

Another weakness of our design is user experience. 3D printing users like to see their prints as they are printing - both out of interest and to monitor printing performance and status. Since our enclosure is made out of opaque insulating material, our design does not allow for this transparency into the print while printing. This can be frustrating for the user. While this opacity design decision was done to decrease prototyping cost, we have ideas to improve the user experience which we will detail in the next section.

Also, our adhesion method did not work as well as we had hoped. In our design, we selected a PEI plate as our build plate adhesion. We hope to plate it on tip of the existing Ender 3 build plate to promote adhesion between the part and the printing bed, a crucial task at the beginning of the print. Unfortunately, the consistency of the surface finish of the PEI plate deteriorated during long prints to the point where it affected the quality of the part as a whole. This was disappointing, but as we later discovered in the final testing which was conducted without the PEI plate, warping was dramatically improved even without this part of our solution.

Early on in the testing phase of our baseline printer, we ran into issues using the CMM as it couldn't read the black filament that we initially had used on the red laser system. We had to order white filament for the printer which cut into our production timeline to get better baseline data. This was ultimately futile, however, since the university stopped allowing access to the CMM while the school locked down.

4.3 Recommended Changes for Future Iterations

We would have changed a few elements in our design and design process to address its weakness and other issues we encountered throughout the semester. First, in order to counter the ease of installation issue for a user that is not as skilled as one of the engineers on the team, we would have liked to replace the Ender 3's build plate system entirely. This would offer a few benefits. First, we could assembly our solution on our own build plate, leaving just the installation of the complete unit to the user. This would also likely provide performance benefits. In addition to the simplification of the installation process the part adhesion issue could be addressed simultaneously. With the incorporation of a adhesive bed on top of our custom conductive bed, we would solve both problems with a more built out solution. One of the design challenges we faced was the placement of the heating elements; we had to find a way to effective control the Ender 3's flawed control system while find space among the Ender 3's equipment. By designing our own build plate, we would bypass these challenges and have more control over the design. An example of the modified design is shown in Figure 30. This design uses a very conductive copper heating bed with a polycarbonate plate on top where the pat prints. Nine heating elements placed in each of the three regions would provide very consistent temperature across the build plate, with a maximum deviation of around $3°C$. This would ostensibly be a more expensive solution, but we think that we could still have been able to control costs to meet our specifications.

Our new build plate control system described above would also help achieve further build plate uniformity which would lead to higher part quality and consistency. However, since there would be 9 heating elements instead of four, they would likely interact, creating a more complicated MIMO system. One way to simplify this is to purchase a smaller number of larger heating elements to reduce the complexity of the control system.

In future iterations, we would also recommend addressing user experience as we think this is very important to our stakeholders. While our construction-grade insulating material provided excellent insulation at a low cost, we recommend modifying it. We could replace this material with a clear but slightly less insulating material such as plexiglass. The thermal conductivity of plexiglass is around 0.18 W/mK compared to the insulation's thermal conductivity of 0.024 W/mK. An a alternative, we could cut out windows in the insulation and replace it with plexiglass to provide viewing access

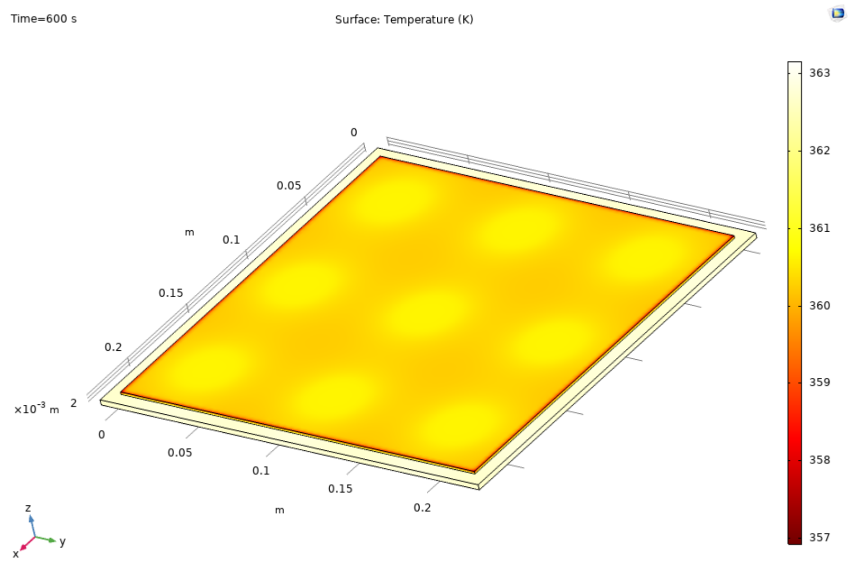

Figure 30: COMSOL Model for New Proposed Build Plate Design

while also keeping most of our cost-effective insulation intact.

Fortunately, most of the pitfalls we encountered helped us develop our solution into a better-designed system. Specifically, we were able to pivot all of our issues detailed above into lessons learned but not necessarily issues that should have been avoided. Framing the problem differently in order to constrain our design space into better specifications would've been helpful. This would have saved us time in creating ideas and moving toward a prototype so that we would've been able to iterate our solution. Most of the issues that we encountered were solved but at the cost of time. The problems encountered with the testing regime, build plate cohesion, and specification ambiguity ultimately lead us to fully develop a design solution, but it would have been helpful to have some foresight on how those would affect us.

4.4 Lessons Learned

We are curious to what extent the decrease in warping is due to the bed control system or the enclosure itself. We would have liked to run more experiments to test these theories. Although, due to the time constraints, as prints are 14 hours long, and the cost associated with purchasing more material, we were not able to test the individual effects.

We are also interested in investigating potential differences in performance between printing a batch of 9 parts versus a batch of 1 part. Throughout all of our testing, we printed batches of 9 parts, one on each region. While industry users likely do this to save time, just like us, they also likely print parts one-at-a-time. Based on our knowledge of the heat transfer phenomena and warping, we believe that printing a batch of nine would pose more quality challenges since there is more time between each layer; the extruder must print a layer on all nine parts before moving on to the next one. Thus we'd expect even better quality results in a single batch trial, but we would like to run an experiment to confirm our hypothesis or encounter any unforeseen phenomena.

We also discovered that the enclosure temperature is much too hot at times. On long prints the heat got up to $60°C$ before we had to cancel it and readjust our system to print on low stilts to allow some heat to escape. We thought that the issue would be that the ambient temperature wouldn't be hot enough, but when in practice, the system was too hot in the enclosure. This system could benefit from adding a venting fan as we had initially thought and left for Phase 3. This was ruled out because we only tested for minimum temperature not max withing the enclosure. Better testing and design criteria should have been used here. Additionally, near the end of our printing of test parts, we discovered a faulty Nozzle temperature regulator which had to be replaced. It was surprising to see that the 3D printer failed before the completion of our parts. More research needs to be done to see if this is due to a faulty system or due to increased heat in the environment. This is concerning because the heating solution we designed hinges on the printer operating more consistently. If our system impairs the durability of the printer that would be cause for concern in the long run. Initially the placement of the heating elements was debated and through COMSOL modeling we determined it to be most effective to place them on the edges instead of the corners as intuition would suggest. This allowed us to control the thermal response in each of the sections, not just the coldest spots. This revelation ultimately made our control gradient the most successful.

4.5 Recommendations for project sponsor

Professor Okwudire: Having met all requirements, we believe that we have sufficiently completed our necessary research and prototyping of our design solution. Included in this report and appendices are all necessary instructions to recreate this if needed or to be expanded upon for future development. Do not hesitate to reach out if you have any questions for us. We recommend that the bed heating system be explored further to determine the dominant control system responsible for improved consistency, whether that be the bed control or the enclosure. Based on our data, we see a statistically significant improvement over current technology. In the future, it would be useful to benchmark the consistency and quality of our solution against higher cost printers. This could quantify our value proposition. Additionally, we feel that our system is important enough to be patentable as we discussed with professor Mazumder and we will be moving forward with that to potentially move to introducing this to market.

5 Conclusion

Having created sufficient design constraints we were able to generate a multitude of ideas through brainstorming to address the most common and detrimental modes of deformation in polymer additive manufacturing. We then evaluated these ideas using design heuristic techniques to refine and broaden our design space. These designs were then formed into a morphological chart to select candidate designs. These designs were evaluated using a Pugh chart ranking system and scored by importance and proficiency. A final design was then selected as a combination of the best features of the candidate designs. Having successfully completed all necessary testing on the base printer, we were able to create a working prototype of our design. We justified the placement and heat transfer modeling of our system for the build plate. We also verified that no further development of the design was needed to control the ambient as this would over-complicate our system for no net benefit. This allowed us to test to see if our design meets our design specifications. We have completed all necessary testing and verification to validate the validity and efficacy of our design. We have created our code for temperature regulation of our heated printing bed as well as the creation of our enclosure. Finally we have completed all necessary printing and measurements to determine the effectiveness of our system and optimized our solution. Our project was very successful in reducing warping and satisfying all of our specifications and requirements from sponsors.

6 Acknowledgements

We are extremely grateful for Professor Mazumder's aid and for continued help from Heather Cooper.

We would also like to extend our deepest gratitude to our project sponsor Professor Chinedum Okwudire.

We would also like to thank Professor Alan Taub for his insight into the topic.

We would also like to thank Professor Albert Shih and Mathew Hildner for guidance.

We would also like to thank Dr. Miki Banu and Jaekwang Shin for allowing access to necessary testing equipment.

We would also like to thank Professor Katsuo Kurabayashi for heat transfer knowledge and consultation.

Special thanks to our stakeholders at Ford and John Deere

7 Authors

Michael Fanelli is a senior studying Mechanical Engineering at the University of Michigan. He is originally from Putnam Valley, New York and is a part of the Engineering Global Leadership Honors Program at Michigan. Over the past two summers, he has interned at Deere & Company in product engineering roles, both in Product Sustainability and Continuous Improvement. He is interested in the intersection between Mechanical and Electrical Engineering and intends to pursue a Master's Degree in Mechanical Engineering, focusing on controls and electromechanical systems.

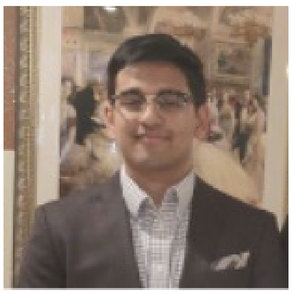

Luthfor Khan is a senior studying Mechanical Engineering at the University of Michigan. His interests are in controls/automation, mechatronics, and interdisciplinary projects. He was raised in Hamtramck, Michigan and had the pleasure to interact learn from individuals from around the world. He enjoys working with the next generation of STEAM students and hopes to grow support for students in his hometown.

Jake Melvin is a senior studying Mechanical Engineering at the University of Michigan. His interests are in hardware design and automation. He is originally from Traverse City, Michigan and has always wanted to go fast. He has extensive engineering internship experience in custom fabrication and product design and realization He hopes to begin his career in national security and defense.

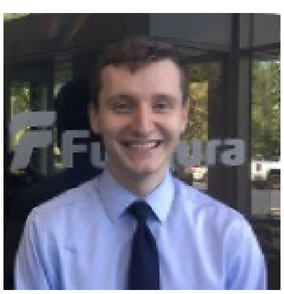

Stefan Milevski is a senior studying Mechanical Engineering at the University of Michigan. His passion for the sciences and helping others brought him to study engineering. His main interests in mechanical engineering lie in design as well as control systems. He was born and raised in southeast Michigan and hopes to help the community that raised him one day. His goal is to have a significant impact on society to help better shape the future. Eventually, he would like to return to academia to pursue both teaching and research.

Hao Wang is a senior studying Mechanical Engineering and Computer Science. He is interested in the general intersection of computer science and mechanical engineering, and more specifically, robotics. He has worked on research projects in areas involving automation and deep learning. Beside doing research, Hao also enjoys teaching and has been involved in instructional roles for three years.

A Mind Maps

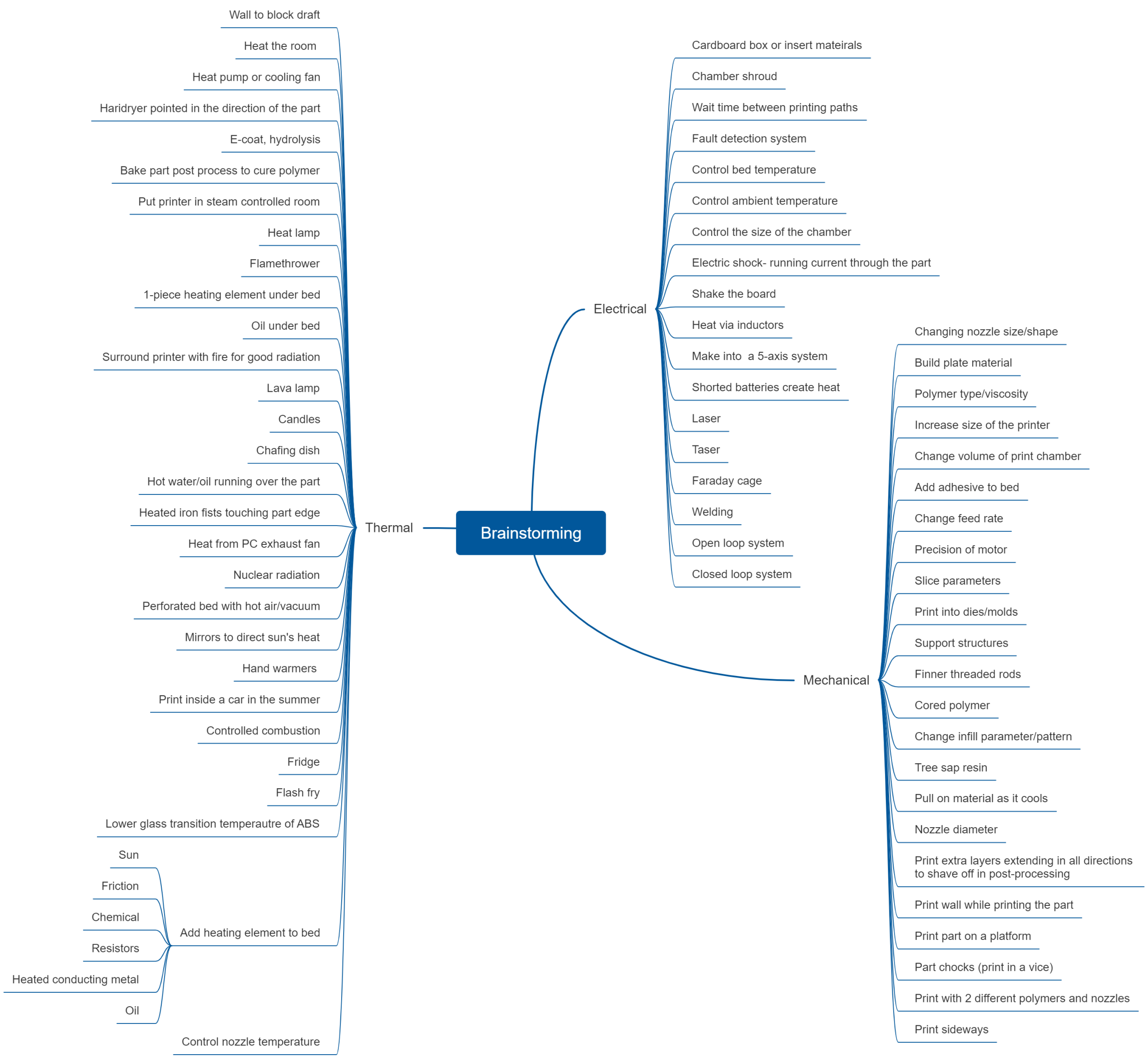

Figure A1: Initial brainstorming session organized into a spatial mind map.

Figure A2: Feasibility of the brainstorming session where red indicates not feasible, yellow indicates somewhat feasible, and green indicates feasible.

B Data Acquisition Wiring Diagrams

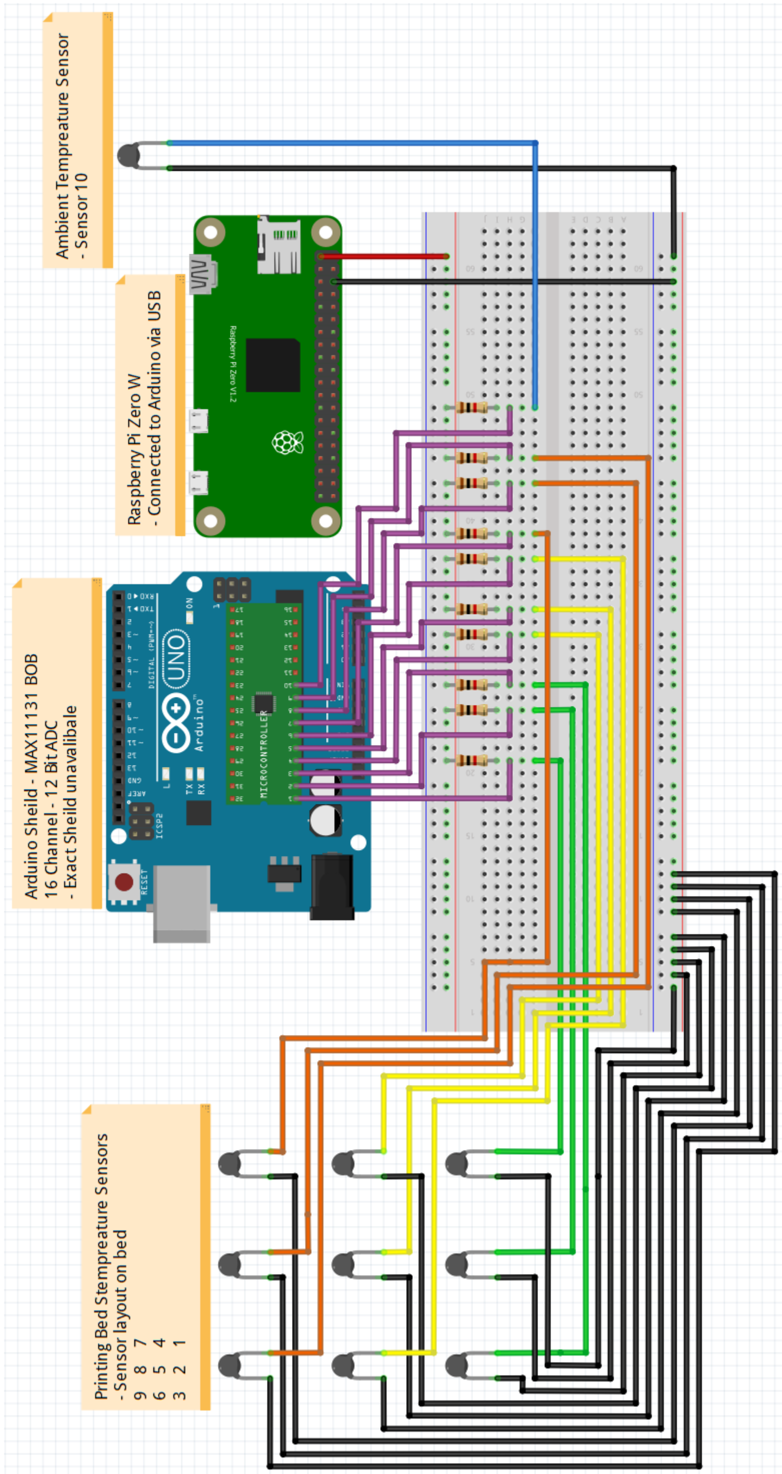

Figure A3: Temperature Data Acquisition Wiring Diagram.

C Heating Element Wiring Diagram

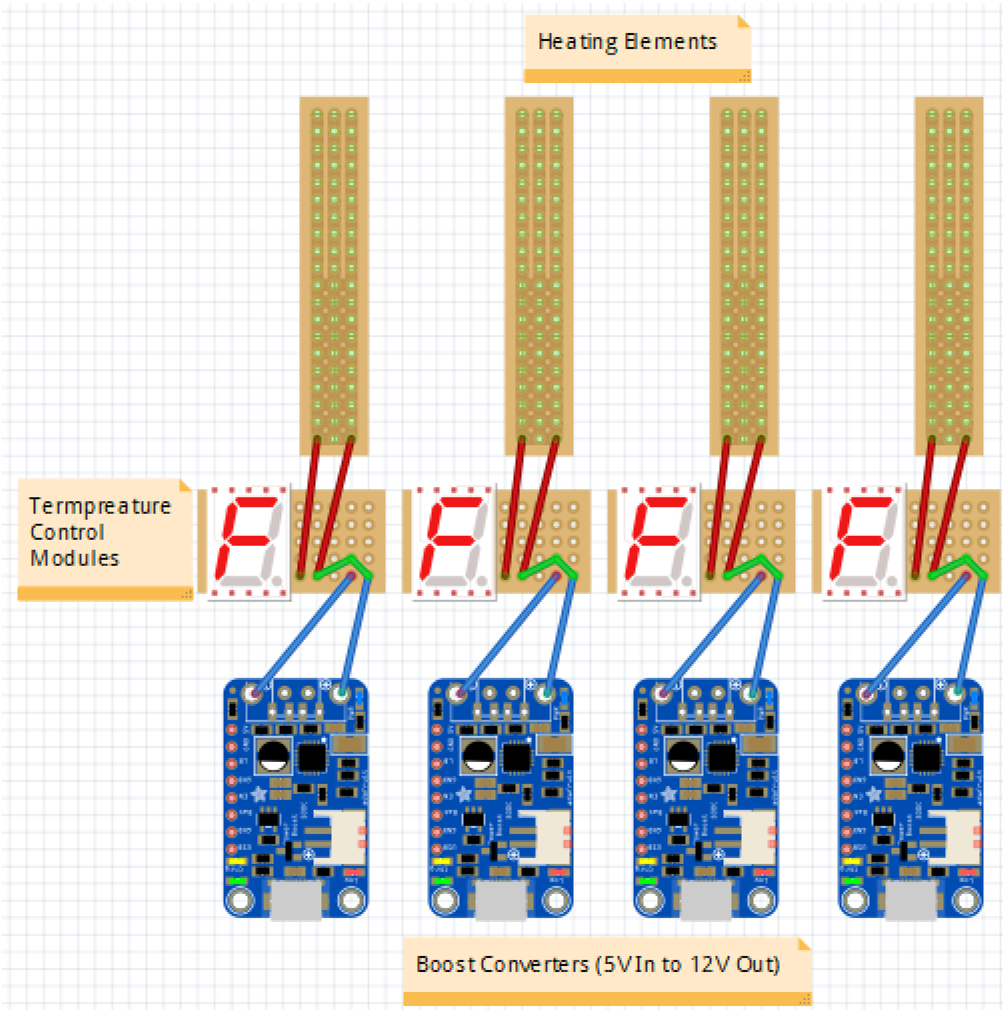

Figure A4: Simplified Heating Element Wiring Diagram.

D Thermal Circuit Analysis

$$q'' = \frac{T_\infty - T_{amb}}{R_{tot}} = \frac{60 - 20}{\frac{1}{10} + 0.528 + \frac{1}{10}} \tag{32}$$

$$q'' = 54.945 \frac{W}{m^2} \tag{33}$$

$$T_\infty - T_i = \frac{q''}{h_i} \tag{34}$$

$$T_i = T_\infty - \frac{q''}{h_i} = 60 - \frac{54.945}{10} = 54.5055°C \tag{35}$$

$$T_\infty - T_0 = \frac{q''}{h_i + R_{th}} \tag{36}$$

$$T_0 = T_\infty - \frac{q''}{h_i + R_{th}} = 60 - 54.945(\frac{1}{10} + 0.528) = 25.495°C \tag{37}$$

E Transient Heat Transfer Model

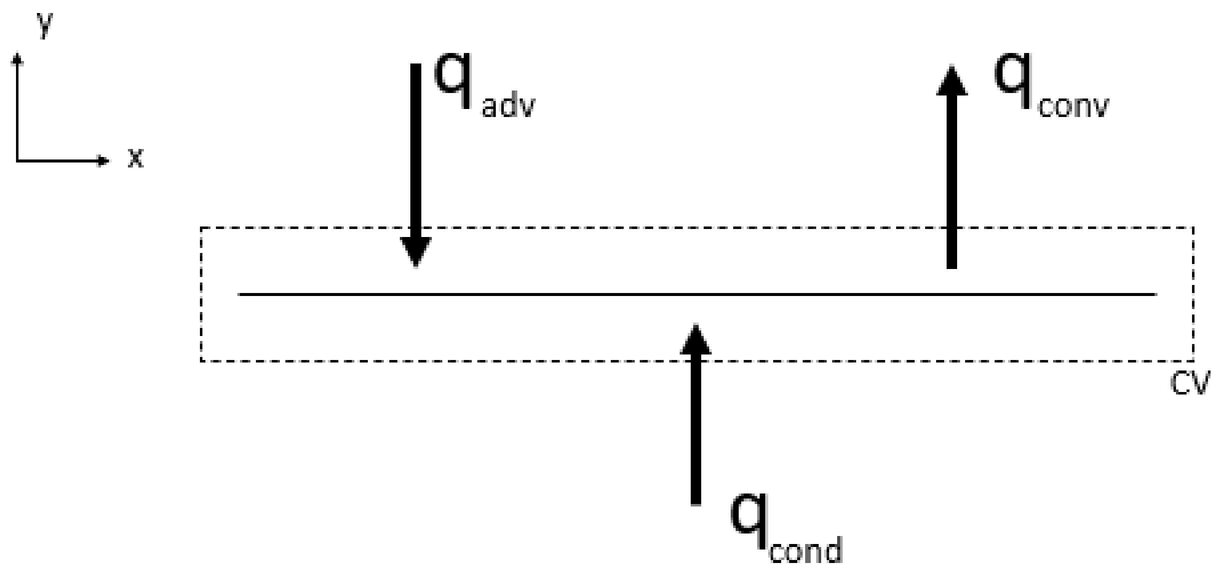

Figure A5: Moving boundary condition

For this model, we will be using the same cube shape in Figure 25. The above image shown above in Figure A5 is the moving boundary layer condition that will be used. This assumptions used in this model is that the cube is being printed a whole layer at a time (this layer being a square). To determine this assumption the following analysis was performed to obtain the volume of the cube as a function of time.

We first defined the number of extrusions needed, N:

$$N = \frac{w}{d} \tag{38}$$

where w is the length of an extrusion and d is the layer thickness.

Next we determined the length of a single layer (m), l_{layer}, with the following:

$$l_l ayer = \frac{w}{d} w \tag{39}$$

Then, the volume of extrusions in 1 layer, Q, was found to be:

$$Q = (\frac{\pi}{4} d^4) l_{layer} \tag{40}$$

We were then able to determine the time required to print a layer (s), as:

$$t_{layer} = \frac{l_{layer}}{r_{ext}} \tag{41}$$

Using a constant cross section, we know the change in height of the cube, h, is a function of time:

$$h(t) = c_1 t + c_2 \tag{42}$$

where c_1 and c_2 are unknown constants, and t is time. The first initial condition is:

$$h(0) = 0 \tag{43}$$

This initial conditions gives us $c_2 = 0$. This tells us that c_1 is equivalent to height multiplied by time. This allows us to define c_1 as:

$$c_1 = \frac{layer}{s}\frac{height}{layer} = \frac{height}{s} \tag{44}$$

From this, we can make substitutions as follows:

$$c_1 = \frac{1}{t_{layer}}d = \frac{r_{ext}}{l_{layer}}d \tag{45}$$

As a result, the height as a function of time was found to be:

$$h(t) = \frac{r_{ext}d}{l_{layer}}t \tag{46}$$

From this we can define the volume, V, as:

$$V(t) = A_c h(t) = w^2 h(t) \tag{47}$$

where A_c is the cross-sectional area of the cube. Simplifying this formula will give us:

$$V(t) = \frac{w^2 r_{ext} d}{l_{layer}}t \tag{48}$$

This gives us the volume of the cube as a function of time. We now may begin control volume analysis of the cube, similar to the one in Figure 25, but now the cube is being built up from the ground. Using the conservation of energy we have:

$$\dot{E}_{cv} = \dot{E}_{in} - \dot{E}_{out} + \cancelto{0}{\dot{E}_g} \tag{49}$$

where $\dot{E}_{cv}$ is the rate of energy storage in the control volume, $\dot{E}_{in}$ is the rate of energy entering the control volume, $\dot{E}_{out}$ is the rate of energy leaving the control volume, and $\dot{E}_G$ is the rate of energy in the control volume. In this case, $\dot{E}_{cv}$ is not 0 as it was found to be in the other analysis. Plugging in the corresponding values gives the following:

$$\rho V c_p \frac{\partial T}{\partial t} = q_{cond,y} - q_{cond,y+dy} - q_{conv} \tag{50}$$

where ρ is the density of the polymer, V is the volume of the polymer , c_p is the specific heat of the polymer, T is the temperature of the part, t is time, k is the thermal conductivity of the part, $q_{cond,y}$ is the thermal conductivity that enters the control volume, $q_{cond,y+dy}$ is the thermal conductivity that exits the control volume, and q_{conv} is the thermal convection that exits the control volume. Using the corresponding values for the values and simplifying gives the following equations:

$$\rho(w^2 dy)c_p \frac{\partial T}{\partial t} = \frac{dq_{cond,y}}{dy}dy - q_{conv} \tag{51}$$

$$\rho c_p w^2 \frac{\partial T}{\partial t} = -kw\frac{\partial^2 T}{\partial t^2} - (4hwdy)(T - T_\infty) \tag{52}$$

$$\rho c_p w \frac{\partial T}{\partial t} = -kw \frac{\partial^2 T}{\partial t^2} - 4h(T - T_\infty) \tag{53}$$

$$kw \frac{\partial^2 T}{\partial t^2} + \rho c_p w \frac{\partial T}{\partial t} + 4h(T - T_\infty) = 0 \tag{54}$$

This equation, Equation 54, is the governing equation for our system. As we can see it is a second order heterogeneous partial differential equation. As a result, we need two boundary conditions and one initial condition. The first boundary condition is easy to solve as we know the temperature of the build plate when the height is zero meters:

$$T(y = 0) = 90°C \tag{55}$$

The next boundary condition needs to be solved using the moving boundary condition problem. This moving boundary condition is seen in Figure A5. Applying the conservation of energy around this boundrary condition yields:

$$\cancelto{0}{\dot{E}_{cv}} = \dot{E}_{in} - \dot{E}_{out} + \cancelto{0}{\dot{E}_g} \tag{56}$$

where $\dot{E}_{cv}$ is the rate of energy storage in the control volume, $\dot{E}_{in}$ is the rate of energy entering the control volume, $\dot{E}_{out}$ is the rate of energy leaving the control volume, and $\dot{E}_G$ is the rate of energy in the control volume. Using the control volume to determine the given heat transfer phenomena gives:

$$0 = q_{adv} - q_{conv} + q_{cond} \tag{57}$$

where q_{adv} is the rate of advection into the control volume, q_{conv} is the rate of convection out of the control volume, and q_{cond} is the rate of conduction into the control volume. Plugging in the corresponding values found above and simplifying will yield the following analysis:

$$0 = \dot{m} c_p T_{adv} - hw^2(T_{adv} - T_\infty) - kw^2 \frac{\partial T}{\partial y} \tag{58}$$

$$\dot{m} c_p T_{adv} = hw^2(T_{adv} - T_\infty) + kw^2 \frac{\partial T}{\partial y} \tag{59}$$

$$\frac{\partial}{\partial t}(\rho V) c_p T_{adv} = hw^2(T_{adv} - T_\infty) + kw^2 \frac{\partial T}{\partial y} \tag{60}$$

$$\rho \frac{\partial V}{\partial t} c_p T_{adv} = hw^2(T_{adv} - T_\infty) + kw^2 \frac{\partial T}{\partial y} \tag{61}$$

$$(\frac{w^2 T_{ext} d}{l_{layer}}) \rho c_p T_{adv} = hw^2(T_{adv} - T_\infty) + kw^2 \frac{\partial T}{\partial y} \tag{62}$$

$$T_{adv}(\frac{\rho c_p r_{ext} d}{l_{layer}} - h) + hT_\infty = k \frac{\partial T}{\partial y} \tag{63}$$

$$\frac{\partial T}{\partial y} = T_{adv}(\frac{\rho c_p r_{ext} d}{l_{layer} k} - \frac{h}{k}) - \frac{h}{k} T_{inf} \tag{64}$$

Equation 64 gives us the boundary condition we need to solve the governing equation. However, after some consultation, we were told to discretize the problem using the following equation:

$$\frac{\partial T}{\partial y} = \frac{T_{adv} - T_{i-1}}{\Delta y} \tag{65}$$

Simplifying the equations yields:

$$\frac{T_{adv} - T_{i-1}}{\Delta y} = T_{adv}(\frac{\rho c_p r_{ext} d}{l_{layer} k} - \frac{h}{k}) - \frac{h}{k} T_{inf} \tag{66}$$

$$T_{i-1} = T_{adv} - \Delta[T_{adv}(\frac{\rho c_p r_{ext} d}{l_{layer} k} - \frac{h}{k}) - \frac{h}{k} T_{inf}] \tag{67}$$

This is our final condition for the moving boundary condition. The last info required is the initial condition which is simply:

$$T(t = 0) = 90^{\circ}C \tag{68}$$

F Project Bill of Materials

Table 6: Project Bill of Materials

Part No.	Part Title	Material	Dimension(s)	Supplier	Quantity	Price	Notes
1	Ender 3		440x410x465mm	Creality	1	$219.41	3d printer
2	Raspberry PI Zero W		66.0x30.5x5.0mm	Raspberry Pi	1	$10.00	Donated
3	ABS Filiment	ABS		Amazon-Basics	2	$41.64	Black and White ABS filiment
4	Thermistors (KTY81/120,112)			Digi-Key	15	$14.63	
5	ADC (MAX11131BOB)			Mouser	1	$11.25	ADC for Analog Devices
6	Arduino Uno		68.6x53.4 mm	Arduino	1	$23.00	Donated
7	HVAC Foil Tape	Aluminum		Lowes	1	$8.58	Bought at Lowes
8	Flexible Polyimide Heating Film (4x)		10x93 mm	Amazon	1	$13.99	
9	Temperature Controller Module			Amazon	4	$14.99	has built in relay and temp sensor
10	Step up Converter			Amazon	1	$11.99	5V to 12V DC Boost converter
11	Micro USB (4x)			Amazon	1	$8.09	
12	12W USB Wall Charger (2 pack)			Amazon	2	$23.98	12 power
13	18 AWG wire	Copper		Amazon	1	$10.98	25 ft red/black wire
14	PEI Sheet	PEI	235mm x 235mm	Amazon	1	$15.95	
15	FOAMULARR-3 Rigid Sheathing	XPS Insulation	1/2 in. x 4 ft. x 8 ft.	Home Depot	1	$10.23	Donated
16	Ender 3 Heating Cartridge			Amazon	1	$10.59	Heating Cartiage Failed
				Budget		$500	
				Total Cost		$449.30	
				Total Donated		$43.23	
				Budget Remaining:		$93.93	

Table 7: Solution Bill of Materials

Part No.	Part Title	Material	Dimension(s)	Supplier	Quantity	Price	Notes
1	HVAC Foil Tape	Aluminum		Lowes	1	$8.58	Bought at Lowes
2	FOAMULARR-3 Rigid Sheathing	XPS Insulation	1/2 in. x 4 ft. x 8 ft.	Home Depot	1	$10.23	Donated
3	PEI Sheet	PEI	235mm x 235mm	Amazon	1	$15.95	
4	Flexible Polyimide Heating Film (4x)		10x93 mm	Amazon	1	$13.99	
5	12W USB Wall Charger (2 pack)			Amazon	2	$23.98	12W power supply
					Solution Cost	$72.73	

G Engineering Standards

In our Problem Definition phase, we explored different engineering standards. We found these standards to be a compilation of subject matter expertise rather than a suite of rigorous testing procedures. Since additive manufacturing is a relatively new technology, it is not heavily standardized. However, technical committees like the ASTM F42 committee continues to work on additive manufacturing standards. Many standards thus far were, in fact, specific to metal additive manufacturing and were not applicable. For example, ASTM F3122-14 (Standard Guide for Evaluating Mechanical Properties of Metal Materials Made via Additive Manufacturing Processes) was not an applicable standard for this project given its focus on metal materials and mechanical properties. However, we did find standards to be useful in our background research. For example, we used standards such as ISO/ASTM 52900:2017 [19] (Additive manufacturing— General principles —Terminology) and ASTM F2792 [20] (Standard Terminology for Additive Manufacturing Technologies) to gain a background on the terms used when speaking about additive manufacturing in technical terms. A standard such as ISO/ASTM 52910:2019 [21] (Additive manufacturing - Design - Requirements, guidelines, and recommendations) helped us define terms such as surface roughness, accuracy, and precision from a design engineering perspective. ISO/ASTM 52901:2018 [22] (Additive manufacturing – General principles – Requirements for purchased AM parts) explains what customers typically look for in a 3D printed part; this was helpful as we tried to understand stakeholder needs better. This standard detailed common industry terms such as process control, tolerances, and surface texture. These terms weren't very new to our team, but standards like this one helped us use these terms in a concise and accurate manner. Our team planned on using ISO/ASTM 52921:2016 (Standard Terminology for Additive Manufacturing—Coordinate Systems and Test Methodologies) and ASTM F2971 (Standard Practice for Reporting Data for Test Specimens Prepared by Additive Manufacturing) [23] in our testing using the CMM machine. However, since we were not able to access the CMM through our validation phase, we were not able to implement the knowledge we gained from this standard. We also intended to use ISO 1101:2017 (Geometrical product specifications (GPS) — Geometrical tolerancing — Tolerances of form, orientation, location, and run-out) [24] as a reference for our GD&T dimensions we intended to measure with the CMM. We were also unable to use this standard in our project outside of our Problem Definition phase.

In summary, the additive manufacturing space is not very standardized currently. Many of the current standards focus on metals 3D printing or on aspects that were outside the scope of this project, such as mechanical properties [25]. We did find many applicable engineering standards, however. Although these standards did not give us much quantitative information, they helped us better understand the additive manufacturing space and stakeholder needs. We had planned on using two testing standards, but our lack of access to the CMM machine halfway through the semester rendered these standards less relevant.

H Engineering Inclusivity

For our project, our team was very interested in practicing inclusive design. From the beginning of our project, we wanted to create a very open space for interacting with stakeholders. After reviewing what we had done this semester, we see that we created an inviting decision-making space. We had asked multiple stakeholders to speak with us and share their feedback on decisions for our project that could impact them. When deciding which stakeholders to meet, we tried to get a broad and diverse set. Additive manufacturing is still a relatively expanding field and a niche one at that. It is also composed of various categories in which left us particularly limited in our outreach as we needed stakeholders who specifically print with polymers. We were able to interact with stakeholders who were in academia and industry as well as 3D printing hobbyists.

When we engaged with our various stakeholders, we wanted to ensure that we adopted a beginner's mindset. From our initial meeting with our project sponsor, we had a pretty good general idea of the problems people face. However, we wanted to make sure we do not influence stakeholders by informing them of a lot of the previous problems we had researched. However, luckily for us, after asking our stakeholders various questions about the problems they faced, they had come to similar conclusions. There was a consensus that using FDM with ABS filament led to quality issues, dimensional uncertainties, and warping problems. Using this beginner's mindset helped us ensure that the problems were occurring across a range of users as well as gave us insights into new ideas.

We also understood how power and identity affected our project. We noticed in some of the meetings that there existed a power dynamic between us and some of our stakeholders. This dynamic ultimately led to the rise of invisible power. At times, we felt hesitant to ask for more clarification on a topic presented to us because we did not want to seem unintelligent. This may have resulted in not understanding everything our stakeholders were telling us and may have distorted what we thought were problems.

We also made sure to realize that as the engineers in the design space, we ultimately decide how the stakeholders' insights are used in defining the problem. As a result, we had looked at our own social identities to ensure that as a team, we did not skew or try to define our problem for ourselves, but from a neutral party in the terms of our stakeholders. We believe that this was easier for our group as our technology isn't necessarily one that changes from user to user as many other design projects can. Similarly, we know that we are graded on the outcome of our project. We had made sure in our process to try and not have this hidden power inhibit the creativity behind our problem-solving process.

After reviewing our approaches, we realize we could have made our design process more inclusive. While we did try to obtain a diverse set of stakeholders, we realized that due to time constraints required to define our problem for the timeline of the project, we were not able to talk to every stakeholder group. This is easier said than done as the number of stakeholders for a project related to 3D printing as a whole would be enormous. Although, if time had permitted, we definitely could have reached out to more groups. Furthermore, we did have a lot of engagement with stakeholders at the beginning of the semester, but that relationship did not hold as strong at the end of the project's lifetime. We could have tried to encourage true co-design with stakeholders through ongoing conversations and consultation. This may have helped our stakeholders give us more information throughout the process as they may have been cautious or unsure about our project during our initial conversations.

I Environmental Context Assessment

After evaluating our solution from an environmental context standpoint, we do believe that our solution does make significant progress towards an unmet and important environmental/social challenge. As we have learned, common environmental consequences from technology include impacts such as smog formation, particular matter emission, or global warming to name a few. The worst effect our design solution has is that it draws a small amount of electrical power from the current electrical grid. It also requires a few parts/materials that take energy to manufacture (heating elements and insulation material). As a result, our design solution has very little impact on these potential environmental consequences. Furthermore, as the world grows, more and more electricity on the grid is going to be renewable and clean. Also, from the results of our solution, we have seen great improvement in consistency and reducing warping. These results mean that, if the solution was adopted, people will waste a lot less material due to failed prints. This is a compounding effect, as the energy inputs required to process the material, transport it, print it, and throw it away can start adding up. These energy inputs can have a very large impact on the environment in terms of emissions and our solution aims at reducing those by increasing printed part quality.

We do not believe there is a potential for the system to lead to undesirable consequences in its lifecycle that overshadow the benefits. The temperature modules are not very intensive electrical parts and they will be able to function for the same duration as the 3D printer itself. The insulation material is even more durable and should outlive the lifetime of the 3D printer. As stated earlier, we believe that during the lifecycle of our solution, it will be able to reduce more emissions than it took to create and dispose of our solution. As a result, we see no way that our system could lead to consequences that would overshadow the environmental benefits in its lifecycle.

J Social Context Assessment

After evaluating our solution from an environmental context standpoint, we do believe that our solution does make significant progress towards an unmet and important environmental/social challenge. As we have learned, common environmental consequences from technology include impacts such as smog formation, particular matter emission, or global warming to name a few. The worst effect our design solution has is that it draws a small amount of electrical power from the current electrical grid. It also requires a few parts/materials that take energy to manufacture (heating elements and insulation material). As a result, our design solution has very little impact on these potential environmental consequences. Furthermore, as the world grows, more and more electricity on the grid is going to be renewable and clean. Also, from the results of our solution, we have seen great improvement in consistency and reducing warping. These results mean that, if the solution was adopted, people will waste a lot less material due to failed prints. This is a compounding effect, as the energy inputs required to process the material, transport it, print it, and throw it away can start adding up. These energy inputs can have a very large impact on the environment in terms of emissions and our solution aims at reducing those by increasing printed part quality.

We do not believe there is a potential for the system to lead to undesirable consequences in its lifecycle that overshadow the benefits. The temperature modules are not very intensive electrical parts and they will be able to function for the same duration as the 3D printer itself. The insulation material is even more durable and should outlive the lifetime of the 3D printer. As stated earlier, we believe that during the lifecycle of our solution, it will be able to reduce more emissions than it took to create and dispose of our solution. As a result, we see no way that our system could lead to consequences that would overshadow their design solution was rooting on a low-cost perspective. We knew that expensive, high-end 3D printers have solved consistency and warping issues, but at a high cost to the consumer. Since many companies are hesitant to make such a large investment, particularly if the company is relatively new to 3D printing, we knew that our solution could be successful in this market. Our stated goal was to make a low-cost kit that can be used on low-cost 3D printers that would raise their quality to that of more expensive printers for a much smaller cost. With this context in mind, our design solution was constructed to be affordable for these low-end and medium-level printers, such as an Ender 3 and an Ultimaker. One feature of our solution is the low-cost materials required. If an area in the world has the ability to purchase a 3D printer and have it delivered to them, then there is a high chance that the parts required for this kit would be readily available and able to be delivered. When comparing this device to other solutions such as the Creality enclosure, we demonstrate a decrease in price. As a result, we believe our system is likely to be adopted and can be self-sustaining in the market. There is a market need and we have demonstrated that we can fill that need through our verification.

Our solution does give us fairly good benefits; however, it fits a particular niche in a large area. Our solution provides users with a low-cost method for addressing warping found in ABS printed parts through FDM. This is generally a problem for lower-end 3D printers, although we believe our solution could improve higher quality models as well. Due to its relative niche demand, we anticipate that our solution will mainly be used in a relatively low amount of scenarios for additive manufacturing applications as a whole. As a result, we do not believe that our solution will be so economically successful that it will hurt planetary or social systems.

The final condition necessary to define sustainable design is the technology's resilience to disruptions in business cycles. In our project's case, the final solution is rather cost-efficient, using a combination of relatively inexpensive and common parts. We think that this product will actually thrive during downturns in business cycles. When budgets are tightened, a business will look for ways to cost-efficiently deliver quality products - our final solution does exactly that. Even during optimistic business environments, we still think our value proposition is strong and companies will still seek thee cost-efficient solutions. Instead of demand, the real risks from business cycle volatility could stem from suppliers going out of business, unstable financing, and competition from better-funded competitors. Given all this, we think our solution is robust and can withstand significant economic disruption.

K Ethical Decision Making

Throughout our project, our team placed a heavy focus on applying ethical decisions in the design process. We were all somewhat familiar with the various codes of ethics for engineers and followed their canons and rules closely. In particular, when looking at the NPSE Code of Ethics for Engineers, we made sure the safety of the public was our top priority. For example, we performed a thermal circuit analysis to ensure that with a hot enclosure, that the outside of the box could be handled safely. Similarly, as the average print time we faced was around 14 hours, we ensured that we gave the printer enough time to cool before prints. This was to keep the printer from running too much and leading to possible thermal overload in which could put users in danger. Finally, we had completed an FMEA to encapture the safety of our project as a whole. The full FMEA is shown in the Appendix. Another aspect of the code is to avoid any deceptive acts. All our data provided is exactly what was found and measured. Nothing has been altered for our benefit, and the results are truly the results of our project.

One of the ethical philosophies our team had a common liking to was utilitarianism. The essence of our project was the idea to help people with common problems that are faced when 3D printing with ABS. When making decisions, we wanted to choose those that created the greatest good for the greatest number of people. In our case, we wanted to ensure that our product was inexpensive and started working up from lower-end desktop 3D printers. Luckily, our stakeholders agreed on this aspect. Furthermore, the greatest good would also arise from an actual functional product. We considered that when choosing a design as shown in our Pugh chart analysis. We had a few unique ideas, and we're considering their application. Although, we decided that while the ideas could function well, we did not have the time and resources available to create a solution that has a high chance to fail. As a result, we went with a solution that we believe has a much higher chance of success.

In terms of ethical dilemmas we faced, we had only really seen the two mentioned above. The first dilemma is displaying the information that we found versus falsifying data to provide an even better solution. Following the code of ethics, avoiding any deceptive acts, and following the Michigan Honor Code, we have provided only data that was found through our experiments. The second dilemma was the decision between making a unique solution that may work but comes with a high chance of failure versus one that is less unique but has a high chance of success. As per our discussion on utilitarianism we have chosen the latter for this project.

L Risk Assessment: FMEA

FMEA Number	Item	Function	Potential Failure Mode	Potential Effect of Failure	Severity	Potential Cause	Occurrence	Current Design Controls	Detection	RPN	Recommended Action
1	ABS Filament	Material the Ender 3 3D printer uses to print the parts	When 3D printed, due to the high temperatures, ABS will release a toxic fume	The toxic fume from the ABS filament can cause discomfort when inhaled	4	Common problem coupled with printing with ABS filament	3	Ventilation system in area that is being 3D printed	4	48	Well ventilated working area
2	Wires	Provides power and communication across the system	Exposed/damaged wires	If the device is being operated and wires have been exposed or broken, the user may experience electric shock	6	Bad/old wires, assembled poorly	3	Low power electronics with insulated connections	3	54	Create PCP with insulated connections and non-conductive casing
3	Heating Module	Provides electricity and feedback control to heating elements	Thermal runoff	Thermal runoff could lead to the module informing the sensors to keep heating the part indefinitely instead of keeping it at a constant temperature	4	Sensor control loop failure	2	Relay shutoff	2	16	Obtain another sensor
4	Heating Elements	Provides heat	Melting plastic near the heating elements	Could potentially lead to a fire	10	Thermal runaway or poor plastic material on heating elements	1	Strong adhesive to keep heating elements secure	1	10	Research higher temperature rated adhesion materials
5	Boost Converter	Increases output voltage	Exposed electric componenets	Possibility of electric shock	6	Exposed electronics and contacts with the power source, user error	2	Currently encased in tubing	4	48	Research alternatives to boost converter for this application
6	Boost Converter	Increases output voltage	Boost converter short circuits	Voltage of the heating modules would not be raised to appropriate levels	8	Improper wiring, electrical components are faulty	2	Proper wiring and inspection intervals	2	32	Ground the entire system to prevent short circuiting
7	Enclosure	Keeps heat inside the enclosure	Outside of enclosure becomes too hot	Interacting with the enclosure at high levels of heat may lead to very small burns	1	Thermal runaway causes the inside temperature to be too hot, user error	4	Wait sufficient time after print ends for the enclosure to cool down	3	12	Provide users with PPE for hands

References

[1] Huang, Y., Leu, M. C., Mazumder, J., and Donmez, A., 2015. "Additive Manufacturing: Current State, Future Potential, Gaps and Needs, and Recommendations". *Journal of Manufacturing Science and Engineering,* ***137***(1), 02. 014001.

[2] Lepoivre, A., Boyard, N., Levy, A., and Sobotka, V., 2020. "Heat transfer and adhesion study for the FFF additive manufacturing process". *Procedia Manufacturing,* ***47***(2019), pp. 948–955.

[3] Costa, A. E., Silva, A. F. D., and Carneiro, O. S., 2019. "A study on extruded filament bonding in fused filament fabrication". *Rapid Prototyping Journal,* ***25***(3), p. 555–565.

[4] Yin, J., Lu, C., Fu, J., Huang, Y., and Zheng, Y., 2018. "Interfacial bonding during multi-material fused deposition modeling (fdm) process due to inter-molecular diffusion". *Materials Design,* ***150***, p. 104–112.

[5] Spoerk, M., Arbeiter, F., Cajner, H., Sapkota, J., and Holzer, C., 2017. "Parametric optimization of intra- and inter-layer strengths in parts produced by extrusion-based additive manufacturing of poly(lactic acid)". *Journal of Applied Polymer Science,* ***134***(41), p. 45401.

[6] Gurrala, P. K., and Regalla, S. P., 2014. "Part strength evolution with bonding between filaments in fused deposition modelling". *Virtual and Physical Prototyping,* ***9***(3), pp. 141–149.

[7] Carneiro, O., Silva, A., and Gomes, R., 2015. "Fused deposition modeling with polypropylene". *Materials Design,* ***83***, pp. 768 – 776.

[8] Wang, T. M., Xi, J. T., and Jin, Y., 2007. "A model research for prototype warp deformation in the FDM process". *International Journal of Advanced Manufacturing Technology,* ***33***(11-12), pp. 1087–1096.

[9] Rodriguez, J. F., Thomas, J. P., and Renaud, J. E., 2000. "Characterization of the mesostructure of fused-deposition acrylonitrile-butadiene-styrene materials". *Rapid Prototyping Journal,* ***6***(3), pp. 175–185.

[10] Turner, B. N., Strong, R., and Gold, S. A., 2014. "A review of melt extrusion additive manufacturing processes: I. process design and modeling". *Rapid Prototyping Journal,* ***20***(3), p. 192–204.

[11] Ravoori, D., Prajapati, H., Talluru, V., Adnan, A., and Jain, A., 2019. "Nozzle-integrated pre-deposition and post-deposition heating of previously deposited layers in polymer extrusion based additive manufacturing". *Additive Manufacturing,* ***28***, Jun, p. 719–726.

[12] Shahrain, M., Didier, T., Lim, G. K., and Qureshi, A. J., 2016. "Fast Deviation Simulation for 'Fused Deposition Modeling' Process". *Procedia CIRP,* ***43***, pp. 327–332.

[13] Costa, S. F., Duarte, F. M., and Covas, J. A., 2015. "Thermal conditions affecting heat transfer in FDM/FFE: a contribution towards the numerical modelling of the process: This paper investigates convection, conduction and radiation phenomena in the filament deposition process". *Virtual and Physical Prototyping,* ***10***(1), pp. 35–46.

[14] Theodore L. Bergman, Adrienne S. Lavine, F. P. I. D. P. D. *Fundamentals of Heat and Mass Transfer.* Wiley.

[15] Yilmaz, S., Daly, S. R., Seifert, C. M., and Gonzalez, R., 2016. "Evidence-based design heuristics for idea generation". *Design Studies,* ***46***, pp. 95–124.

[16] Mahesh, M., Wong, Y., Fuh, J., and Loh, H., 2004. "Benchmarking for comparative evaluation of rp systems and processes". *Rapid Prototyping Journal,* ***10***(2), p. 123–135.

[17] Rebaioli, L., and Fassi, I., 2017. "A review on benchmark artifacts for evaluating the geometrical performance of additive manufacturing processes". *The International Journal of Advanced Manufacturing Technology,* ***93***, Jul, p. 2571–2598.

[18] Sanchez, F. A. C., Boudaoud, H., Muller, L., and Camargo, M., 2014. "Towards a standard experimental protocol for open source additive manufacturing". *Virtual and Physical Prototyping,* ***9***(3), p. 151–167.

[19] BS EN ISO/ASTM 52900:2017, 2017. Additive Manufacturing – General Principles – Terminology. Standard, British Standard Institution.

[20] ASTM F2792-12a, 2012. Standard Terminology for Additive Manufacturing Technologies (Withdrawn 2015). Standard, ASTM International, West Conshohocken, PA.

[21] BS EN ISO/ASTM 52910:2019, 2019. Additive Manufacturing -Design-Requirements, Guidelines and Recommendations. Standard, British Standard Institution.

[22] BS EN ISO/ASTM 52901:2018, 2018. Additive Manufacturing – General Principles – Requirements for Purchased. Standard, British Standard Institution.

[23] ASTM F2971-13, 2014. Standard Practice for Reporting Data for Test Specimens Prepared by Additive Manufacturing. Standard, ASTM International, West Conshohocken, PA.

[24] BS EN ISO 13586:2017(E), 2017. Geometric Product Specifications – Geometrical Tolerancing – Tolerances of Form, Orientation, Location and Run-Out. Standard, British Standard Institution.

[25] Gibson, I., Rosen, D. W., and Stucker, B., 2010. *Additive Manufacturing Technologies: Rapid Prototyping to Direct Digital Manufacturing.* Springer.